

FOLIO
TA 7
C 6
1964
no. 37
cop. 2

SCIENCES

AN EXPERIMENTAL STUDY OF TURBULENT
BOUNDARY LAYER STRUCTURE

by

E. J. Plate and V. A. Sandborn

Final Report on U.S. Army Research Grant
DA-SIG-36-039-62-G24

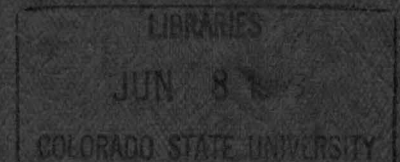
with

Meteorology Department
U.S. Army Electronic Research and Development Activity
Fort Huachuca, Arizona

Fluid Dynamics and Diffusion Laboratory
Colorado State University
Fort Collins, Colorado

December 1964

CER64EJP-VAS37



AN EXPERIMENTAL STUDY OF TURBULENT
BOUNDARY LAYER STRUCTURE

by

E. J. Plate and V. A. Sandborn

Final Report on U.S. Army Research Grant
DA-SIG-36-039-62-G24
with
Meteorology Department
U.S. Army Electronic Research and Development Activity
Fort Huachuca, Arizona

Fluid Dynamics and Diffusion Laboratory
Colorado State University
Fort Collins, Colorado

December 1964

CER64EJP-VAS37

TABLE OF CONTENTS

<u>Chapter</u>		<u>Page</u>
I	INTRODUCTION	1
II	EXPERIMENTAL EQUIPMENT AND PRO - CEDURES	1
	2.1 Techniques for measuring mean velocities . .	2
	2.2 The transient response of thermocouples . . .	4
	2.21 Results	7
	2.3 Temperature measurement with resistance thermometers	12
	2.4 Instrumentation for measurement of velocity and temperature fluctuations	12
	2.41 Hot wire evaluation in a turbulent temperature velocity field	13
	2.42 Evaluation of the turbulent velocities normal to the mean flow	18
	2.5 Pressure measurements on rough surfaces . .	24
	2.6 The calibration of the wind tunnel	25
	2.61 Mean velocity calibration	25
	2.62 Turbulent intensity calibration	27
	2.63 Air temperature calibration	31
	2.64 Plate temperature calibrations	31
III	EXPERIMENTS ON VELOCITY DISTRIBUTIONS OVER NEUTRAL BOUNDARIES	34
	3.1 Velocity distributions over smooth boundaries	34
	3.2 Velocity distributions over sand roughened boundaries	40
	3.3 Velocity distributions inside and above flexible roughness	42
IV	EXPERIMENTS ON VELOCITY DISTRIBUTIONS OVER HEATED BOUNDARIES	44

I. INTRODUCTION

This report covers work done in preparation for a systematic investigation of the nature of aerodynamic roughness, and of the effect of thermal stratification on the turbulence structure in forced convection environments over rough and smooth surfaces.

The investigations are based on data taken in the U.S. Army meteorological wind tunnel, which has recently been put into operation at Colorado State University. The tunnel had never been checked out thoroughly before beginning of the work reported on, and a large portion of the available time was spent on the initial set up of the wind tunnel. After completion of the tunnel check out, exploratory measurements were made of the distributions of velocity and temperature in a thermally stratified flow (of unstable stratification) and of the velocity profiles above small sample plates covered with different types of sand roughness. A study of the flow of air over flexible roughness was the first comprehensive study which lead to definite conclusions.

While the wind tunnel was readied for experimental work, side studies were undertaken for developing techniques for measuring profiles of mean velocities and mean temperatures, and for measuring fluctuations of temperatures and of velocities.

II. EXPERIMENTAL EQUIPMENT AND PROCEDURES

The experiments reported on were all performed in the U.S. Army Micrometeorological Wind Tunnel Facility which had been constructed

especially for this purpose. The wind tunnel is fully described in a report by Plate and Cermak¹, and for the details of the wind tunnel reference is made to that report. In this chapter, only those techniques and test procedures are described which are different from, or improvements of the techniques described in the report reference.

2.1 Techniques for measuring mean velocities

In the large boundary layers encountered in the meteorological wind tunnel it is found adequate to measure velocities with a pitot-static tube. The tubes used had an outside diameter of 3/16". They were fastened to a probe positioner on which the probe could travel in the vertical direction, as shown in Fig. 2-1. The probe positioner screw is motor driven which permits to remotely place the pitot-static probe at any distance from the floor up to approximately 18".

Initially, the distance from the floor was read from a counter which counted revolutions of the activator. The pressure difference between total and static pressure was read from a water micromanometer type MM-2, made by the Flow Corporation. It was soon found that this technique resulted in a very slow accumulation of data. Therefore, the technique was changed, especially in view of the fact that for purposes of calibration

¹E. Plate and J. E. Cermak (1963) "Micrometeorological wind tunnel facility: description and characteristics "Final Report on Contract DA-36-039-SC-80371 with Meteorology Dept., U.S. Army Electronic Research and Development Agency, Fort Huachuca, Arizona, Report CER63EJP-JEC9, Fluid Dynamics and Diffusion Laboratory, Colo. State Univ., Fort Collins, Colorado.

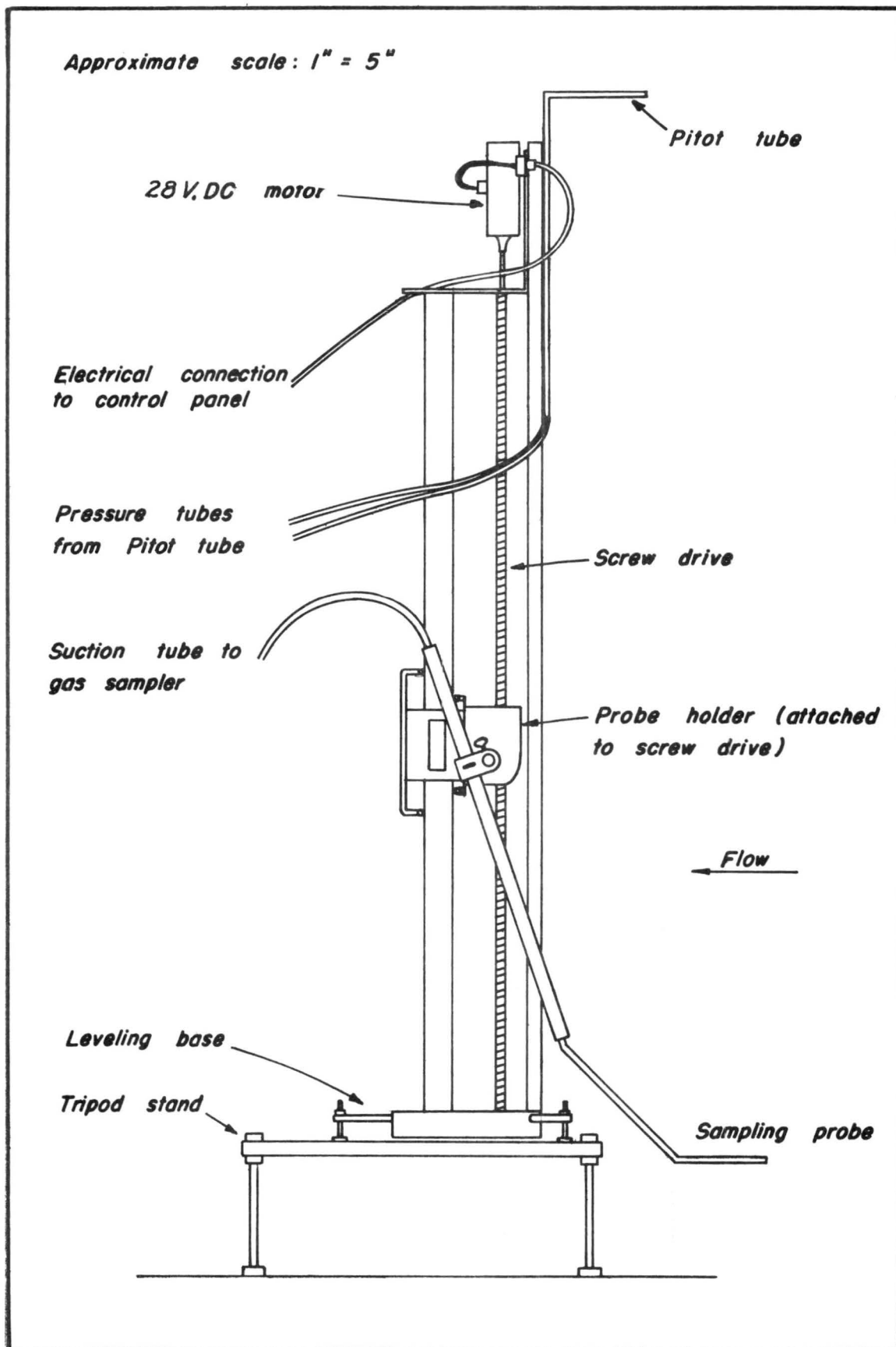


FIG. 2-1 SCHEMATIC DIAGRAM OF TRAVERSING MECHANISM

of the wind tunnel a visual comparison of velocity profiles in adjacent sections became most desirable.

The technique employed then was to plot out the profiles of the dynamic head on an x-y-recorder. The dynamic head was measured with a Transonics Equibar Type 120 electronic manometer which has 8 ranges of pressures from 0.01 mm Hg to 30 mm Hg, with a dc-output, corresponding to each full scale reading, of 30 mv. The voltage corresponding to the pressure was plotted on the y-axis of a Moseley Type 135 x-y-plotter. To the other axis of the x-y-plotter a voltage was applied which corresponded to the voltage drop between wiper and winding of a ten turn potentiometer which was fastened to the probe holder and connected through friction to the vertical support member of the probe actuator. A 1.5 V battery was connected across the potentiometer. In this manner it became possible to plot out continuous profiles of the dynamic head on transparent graph paper, so that profiles could easily be compared by superimposing the traces. A typical example is shown in Fig. 2-2. Turbulent intensity profiles were obtained by the same recording technique, with an example shown in Fig. 2-3.

2.2 The transient response of thermocouples

The laboratory techniques considered for measuring temperature profiles involve continuous motion of a thermocouple junction through the temperature field to be measured. This procedure may give rise to two potential sources of errors. The first error comes about through the

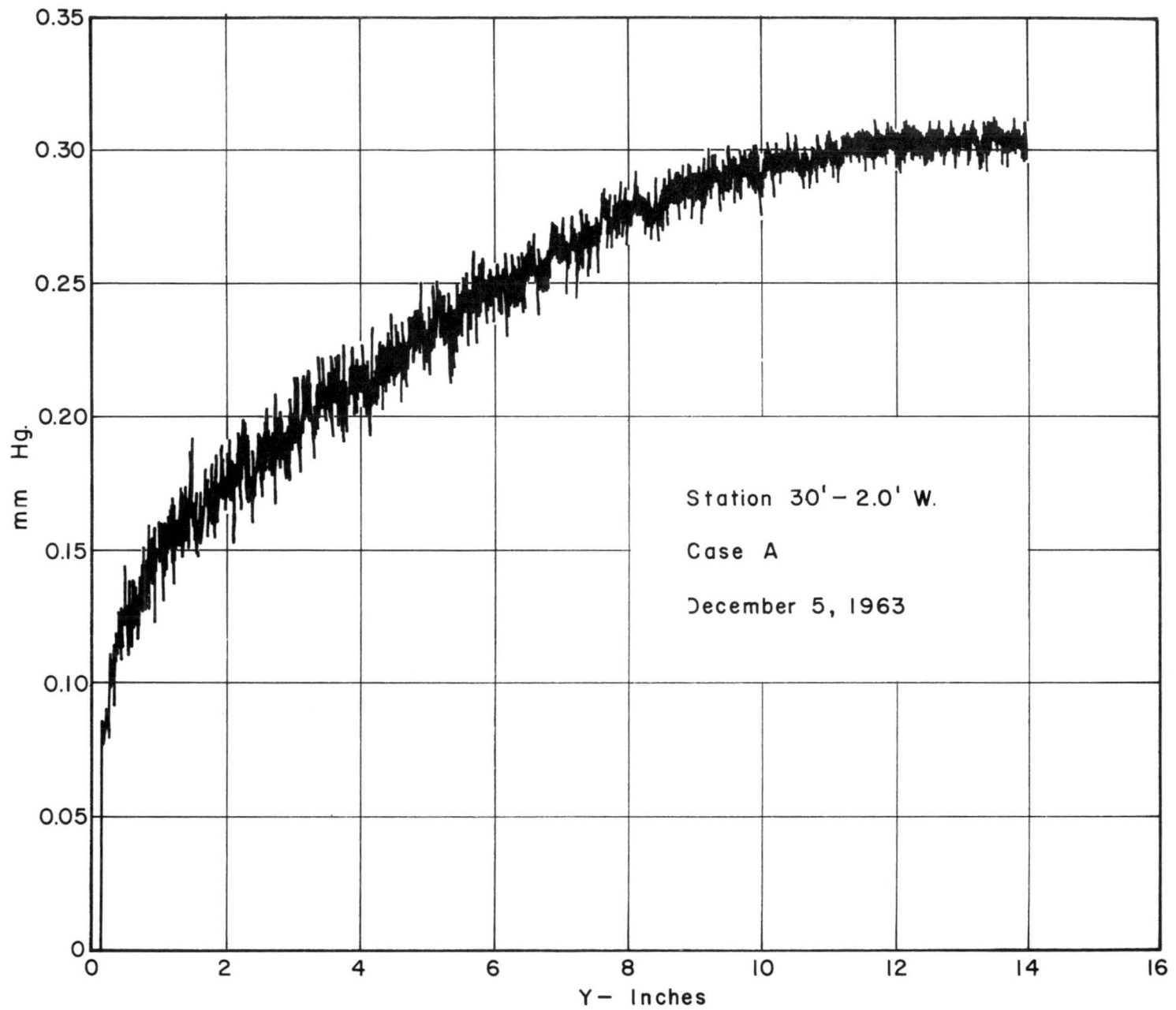


FIG. 2-2 EXAMPLE OF VELOCITY PROFILE TRACE

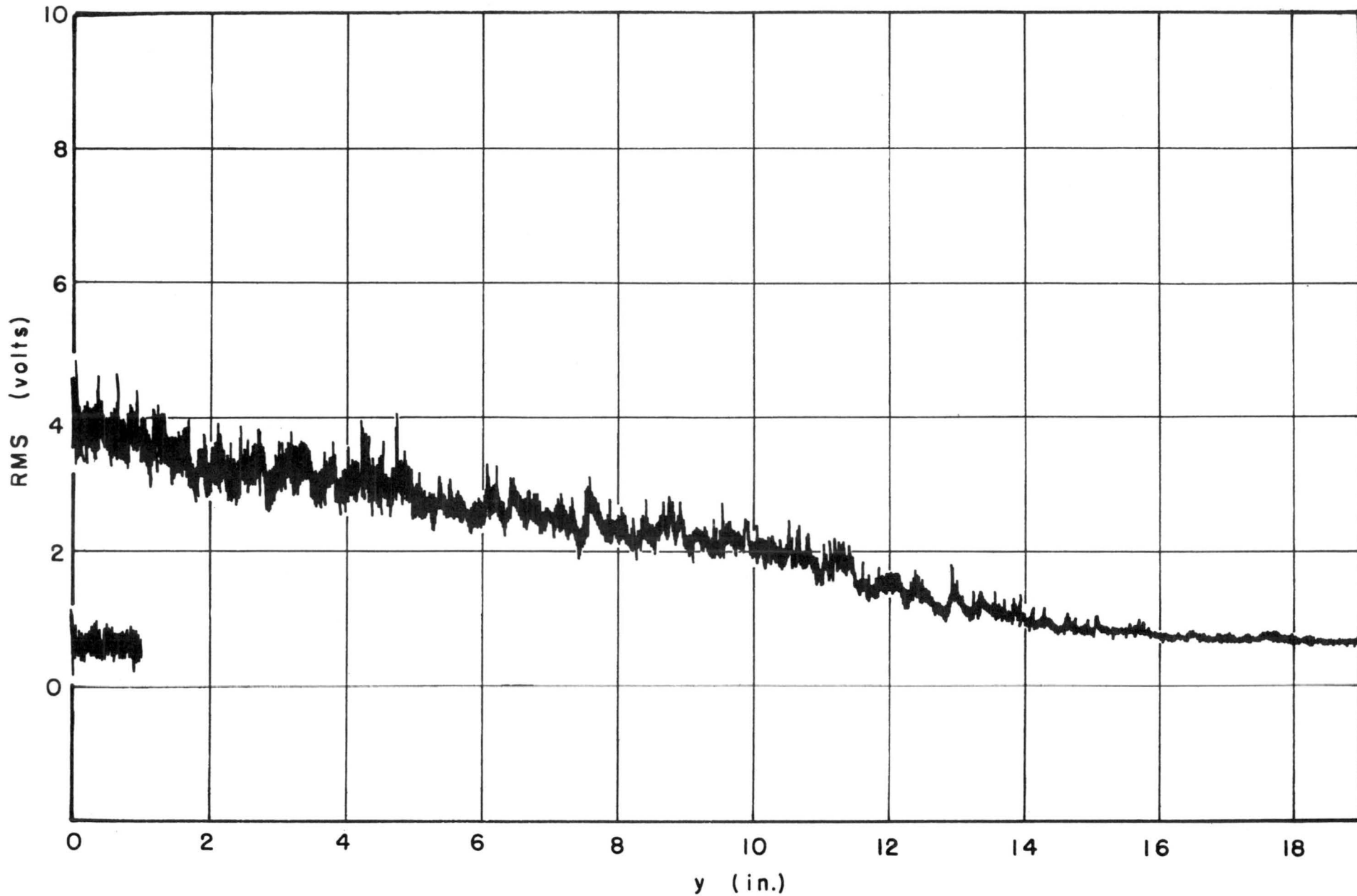


FIG. 2-3 EXAMPLE OF TURBULENT INTENSITY PROFILE





motion of the thermocouple between zones of different temperatures. This will cause a transient effect, with a transient time during which the thermocouple adapts to the temperature of the new environment. The second error results from the possibility of non-uniform heating along the length of the thermocouple wire. This effect changes the conduction of heat away from the junction so that the thermocouple junction may be at a different temperature than the flow at the point where measurements are taken.

In order to obtain some indication on the response characteristics of the thermocouple junction, tests were performed with a step input of heat. The heat source consisted of a heated jet of air coming from an air blower type Master Model AH-501. The blower had an outlet orifice of 1/2".

All thermocouples consisted of copper-constantan junctions made from 26-gage wire ($d = 0.0181$ in.). They were made with different types of junctions as shown in Table 1. The thermocouples were connected to a potentiometer strip chart recorder (Minneapolis - Honeywell Model Brown Y153 x 12) with a range from 0 to 350°F.

2.21 Results--Since the heated jet did not produce a uniform temperature field it was difficult to obtain the true magnitude of the steady temperature at a point in the flow. It was therefore assumed that under equilibrium conditions all junctions should read the same temperatures at the same point. Then differences in the behavior of the individual couples are

TABLE 1: Types of thermocouple junction tested and results

No.	Junction type	Figure	Time constant with lead at room temp.	Time constant with 10 cm lead heated
1	Wires twisted together and welded with insulation (only tip exposed)		19	----
2	Wires twisted together and welded without insulation		4.4	----
3	Junction butt welded without insulation		4.2	10
4	Wires lapped 1 cm and welded without insulation		7	10.8
5	Wires lapped 1 cm and formed into a loop, without insulation		6	10

caused only by transient phenomena, and the effect of leads subjected to temperature changes would result in a different conduction loss from the junction to the leads for different types of temperature gradients along the leads. Clearly, the most severe case is obtained when the leads are subjected to the same temperature changes as the junction, and the most favorable case is obtained if the leads are always in a flow of the same temperature. Therefore, two series of tests were performed. In one series, the junction only was exposed to the hot jet, and the response characteristics were determined. In the second series, a lead wire length of 10 cm and the junction together were inserted into the hot jet. In this manner, some qualitative values can be obtained which permit to consider the effect of conduction on the thermocouple response.

For the response of the junctions without changes in lead temperature, it can be assumed that the thermocouple response can be expressed as a first order system response. It is well known (see Appendix 1) that the differential equation governing the thermal response of a circular wire is given to

$$\rho c_p \frac{\pi d^2 \ell}{4} \frac{d\theta}{dt} + kd\ell\theta = 0 \quad (2-1)$$

where ρ is the density, c_p the specific heat, d the diameter and ℓ the length of the wire, while θ is the difference in temperature between the air and the wire, and k is the coefficient of heat transfer for convective heat transfer. The response can be described by the time constant

$$T = \frac{\rho c_p}{k} \frac{\pi}{4} d \quad (2-2)$$

which is the time required from the beginning of a step change to that point where the temperature difference θ has reached 63% of its final value. The time constant is a good measure for the time which it takes to get a reading of given accuracy at a point.

The coefficient of heat transfer is increasing with increase in the velocity of the air, so that the longest time constant with which one has to count in experimental work is the time constant obtained by letting the wire be heated (or cooled) in still air. Therefore, the tests were made by first placing the junction into the hot air jet, and then suddenly withdrawing the junction into still air. All time constants were obtained in this manner. A sample experiment is shown in Fig. 2-4. The time constant T was found by finding the time which elapses from the beginning of the experiment until the temperature has dropped by 63% of the total range of temperature change. Also shown is the curve which is obtained by assuming first order response with the calculated time constant. The agreement is indeed quite good, which is not surprising since all conductive effects can be lumped into an "effective thermal mass."

The results of the calculations of T for different wire configurations are tabulated in Table 1. It seems that the junctions with lapped ends (4 and 5) have larger time constants than the butt welded and twisted type. Insulation increases the time constant significantly, and so does heating of the wire leads. It is seen from Eq. 2 that the time constant is proportional to d , so that the following conclusion can be obtained from the experiments and the calculations:

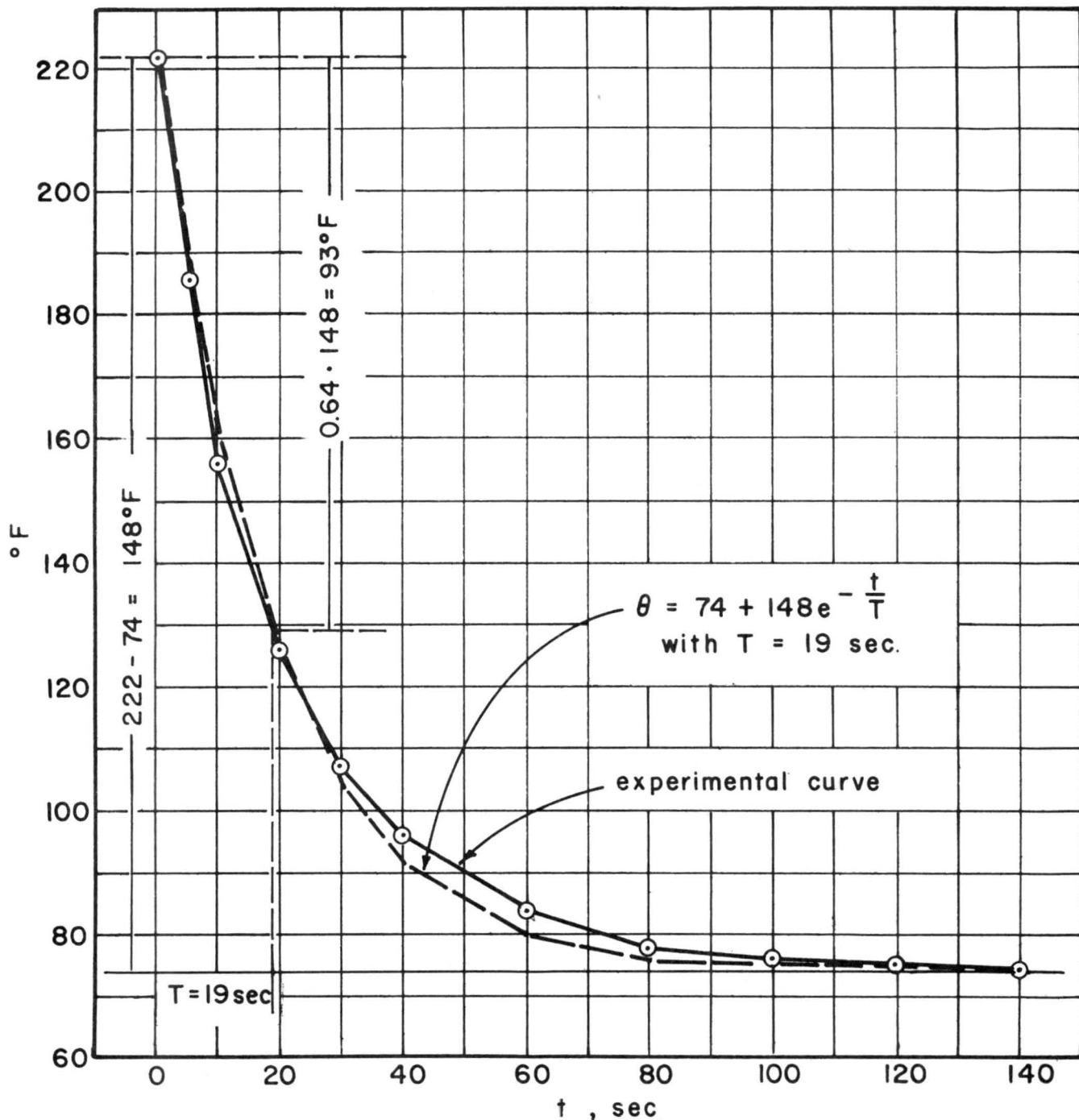


FIG. 2-4 DETERMINATION OF TIME CONSTANT
(example: junction type I)

- a. for application to continuous profile recording, the thermocouples should be as thin as possible.
- b. the thermocouple leads should not be insulated but exposed to the air.
- c. a significant influence of the thermal mass of the leads will be felt in the time constant; the thermocouple response should therefore be determined before each experiment. This is advantageous because the beneficial effect of the air flow on reducing the time constant can be utilized to full advantage.

2.3 Temperature measurement with resistance thermometers

In order to improve the speed of temperature measurement a resistance thermometer probe for measuring fluctuating temperatures was developed. The results, which show the applicability of the resistance thermometer to the measurements contemplated under the Army program, have been reported in the Colorado State University Fluid Mechanics Paper No. 1 by Chao and Sandborn. Their paper is attached to the report as Appendix 1.

2.4 Instrumentation for measurement of velocity and temperature fluctuations

Resistance-temperature transducers were developed to measure the fluctuating temperatures and velocities encountered in the thermal boundary layer. These transducers are a resistance thermometer and a hot wire anemometer. Three specific turbulent terms are of major importance

in the thermal boundary layer. They are: (1) the longitudinal turbulent velocity, (2) the temperature fluctuation, and (3) the correlation between the longitudinal velocity and temperature fluctuation. The turbulent velocity fluctuations in the directions normal to the flow are also of interest. The temperature fluctuations can be measured directly with the resistance thermometer. The velocity fluctuations can be measured directly, and special hot wire anemometer techniques have been developed to allow evaluations of the fluctuating velocities.

The resistance thermometer developed to measure temperature fluctuations is reported in reference 2, which is included as appendix 1 of this report. The evaluation of the hot wire anemometer in a fluctuating turbulent temperature and velocity field is reviewed herein.

2.41 Hot wire evaluation in a turbulent temperature velocity field. -- Experimental evaluation of the heat loss from a hot wire indicates it is a function of fluid temperature, velocity and density. In other words the hot wire can respond as an anemometer, resistance thermometer and a manometer. Thus, a hot wire operating in a thermal boundary layer may respond to both temperature and velocity fluctuations. The hot wire would also respond to density fluctuations if they are present. The present discussion is concerned with only the case where density fluctuations can be neglected. Whether such a case actually exists has by no means been established.

The heat loss from a hot wire may be expressed in terms of a non-dimensional Nusselt number Nu . If the hot wire is heated to a temperature

²Chao, J. L. and Sandborn, V. A.: A resistance thermometer for transient temperature measurements. Colorado State University Fluid Mechanics Paper No. 1.

greater than the surrounding fluid by passing a current through the wire, then the relation between the heating current and the Nusselt number is

$$I^2 R = \pi \lambda k (T_w - \eta T_t) Nu \quad (2-3)$$

where I is the current, R is the hot wire resistance, λ is the length of the hot wire, k is the thermal conductivity of the fluid, T_w is the temperature of the hot wire, η is the recovery temperature ratio for the wire in a given flow (T_e/T_t) and T_t is the total temperature of the fluid. For flows to be considered in the present wind tunnel the recovery temperature ratio is nearly one and the total temperature is equal to the fluid static temperature. (For flows with Mach number approaching 0.5 and above η and T_t must be considered.) Differentiation of equation (2-3) gives (for the case $T_w =$ constant and thus $R =$ constant)

$$2 IR dI = \pi \lambda k (T_w - T) \frac{\partial Nu}{\partial V} dV + \pi \lambda k \left[(T_w - T) \frac{\partial Nu}{\partial T} - Nu \right] dT \quad (2-4)$$

where V is the velocity of the fluid flowing past the wire. Equation (2-4) also neglects the variation of thermal conductivity with temperature. If large variations in temperature are considered then the variation of thermal conductivity must be considered. The variation of density is also neglected in equation (2-4). A further simplification is the assumption that the angle between the wire and the mean flow does not vary. Equation (2-4) can be written in terms of the measured electrical quantities $E = IR$ and $RdI = de$ as

$$de = \frac{\partial E}{\partial V} dV + \frac{\partial E}{\partial T} dT \quad (2-5)$$

Thus, equation (2-5) indicates that for a hot wire held at constant temperature (electronically), it is necessary to know the variation in wire voltage with flow temperature and velocity. For the case of the resistance thermometer it is possible to operate the "hot wire" at such a low value of current (low temperature) that $\partial E/\partial V = 0$ and equation (2-5) becomes

$$\text{RESISTANCE THERMOMETER } de = \frac{\partial E}{\partial T} dT \quad (I \approx 0) \quad (2-6)$$

The possibility was advanced that $\partial E/\partial T$ does not vary with increase in wire temperature, whereas $\frac{\partial E}{\partial V}$ increase rapidly with wire temperature. Thus, by operating the hot wire at high temperatures it might be possible to reach a condition where $\frac{\partial E}{\partial V} \gg \frac{\partial E}{\partial T}$.

Figure 2-5 is a plot of the velocity and temperature sensitivity terms obtained for a 0.0002 inch diameter 90 percent platinum 10 percent rhodium hot wire. The terms are plotted as $\frac{\partial E^2}{\partial V}$ and $\frac{\partial E^2}{\partial T}$ as a matter of convenience only. For the terms plotted in figure 2-5 equation (2-5) would be written as

$$2E de = \frac{\partial E^2}{\partial V} dV + \frac{\partial E^2}{\partial T} dT \quad (2-5a)$$

These data were obtained by placing the wire normal to the flow in a constant temperature stream. The temperature of the wire, rather than the air temperature was varied. It is known, ref. 3 that the heat loss is a function of $(T_w - T)$ rather than the absolute temperature level, so a change in wire temperature is equivalent to a change in fluid temperature (the sign of the sensitivity is reversed). Figure 2-5a shows the velocity sensitivity term,

³Baldwin, L. V.: Slip flow heat transfer from cylinders in subsonic airstreams. NACA TN 4369.

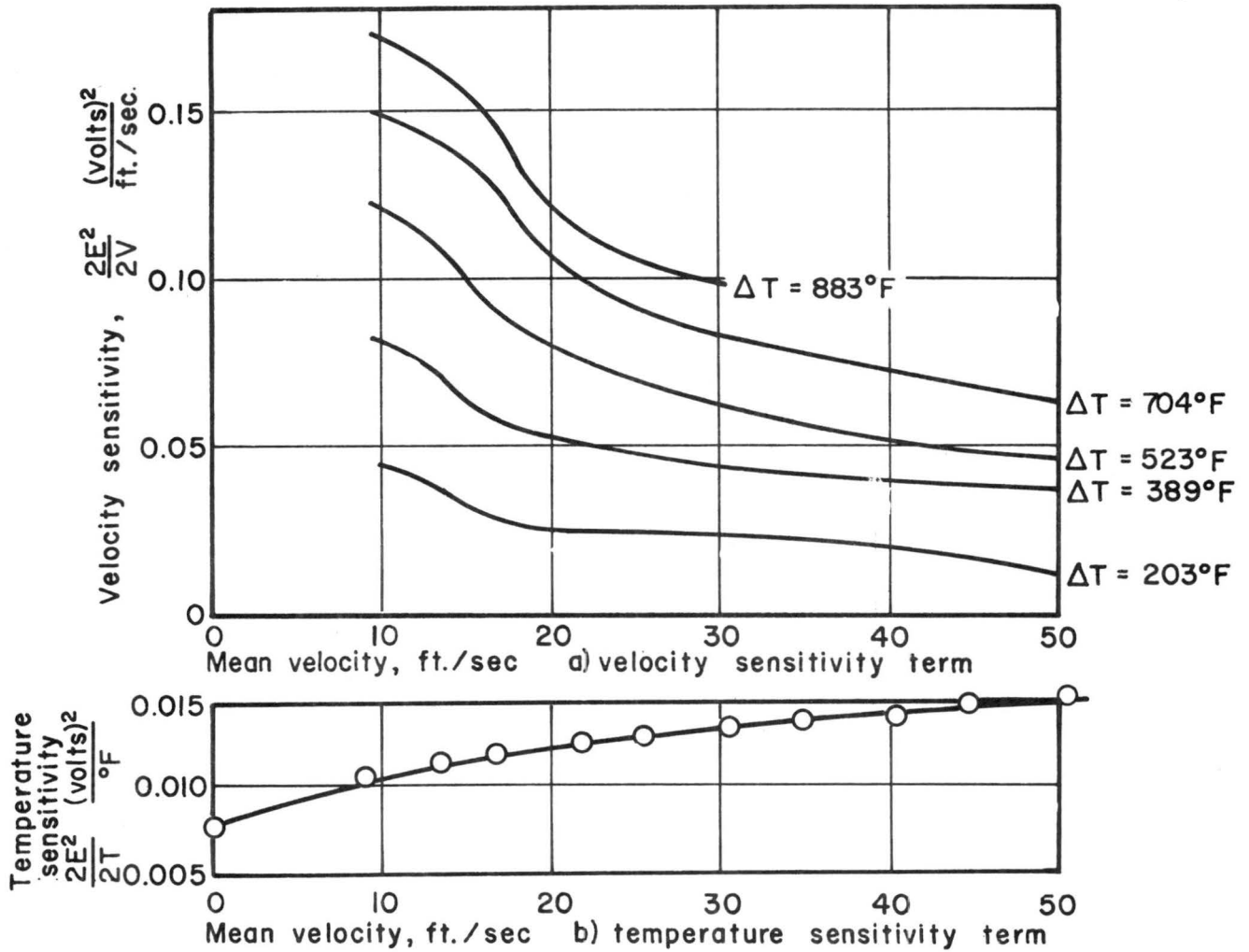


FIG.2-5 EVALUATION OF THE FLUCTUATION SENSITIVITY TERMS AS A FUNCTION OF MEAN VELOCITY AND TEMPERATURE DIFFERENCE

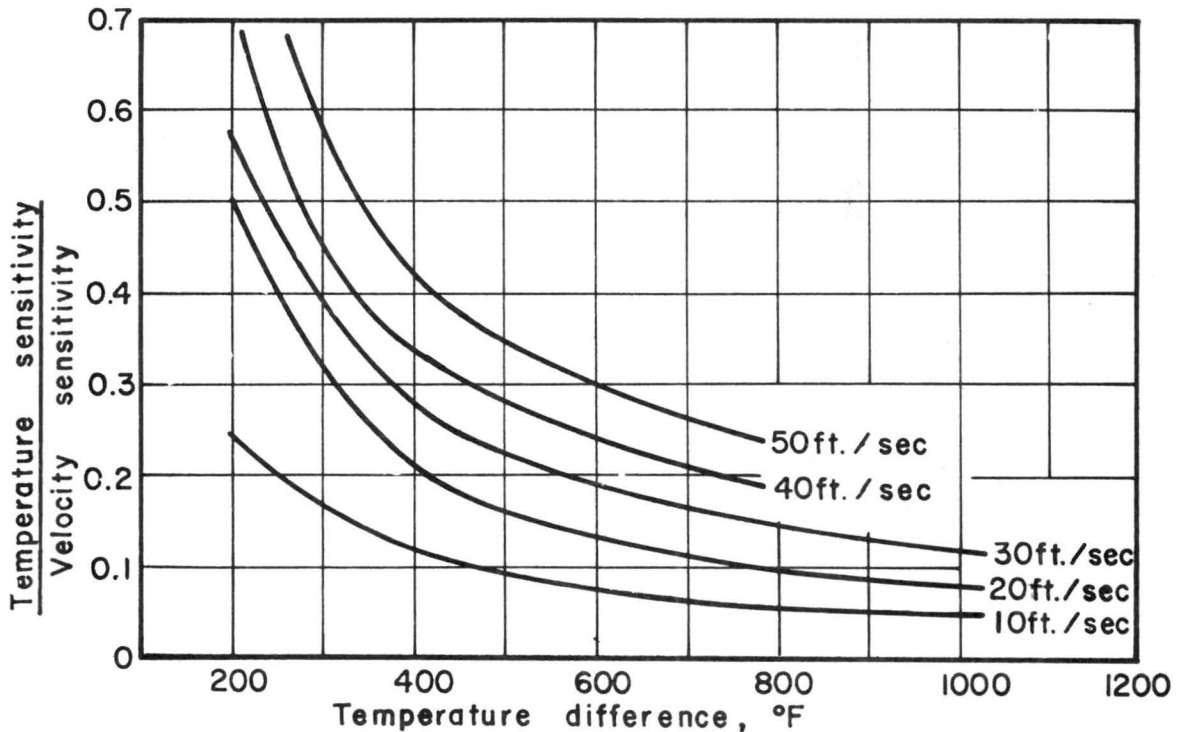


FIG.2-6 COMPARISON OF THE TEMPERATURE AND VELOCITY SENSITIVITIES

which is a function of both ΔT and flow velocity. The velocity sensitivity is greatest at lower velocities and highest ΔT . The temperature sensitivity is not a measurable function of ΔT , however there is a variation with velocity. The variation of the temperature sensitivity with velocity is due mainly to heat conduction to the supports. An infinitely long wire would show a lesser variation with velocity.

Figure 2-6 compares the temperature sensitivity to the velocity sensitivity as a function of ΔT and velocity. In order to neglect the temperature sensitivity it would be desired that an error of less than 5 percent were made. Only the 10 feet/sec case at $\Delta T = 1000^{\circ} \text{F}$ failed to show any marked improvement in the ratio. (The curves are nearly constant values above $\Delta T = 1200^{\circ} \text{F}$.) No means of improving the results of figure 2-6 have been found.

The differentials de , dV and dT are replaced by perturbation quantities $\overline{e^2}$, $\overline{u^2}$ and $\overline{t^2}$. This is equivalent to linearizing the hot wire response equation. Equation (2-5) in terms of the squared quantities is

$$\overline{u^2} = \left(\frac{\partial E}{\partial V} \right)^2 \overline{u^2} + 2 \left(\frac{\partial E}{\partial V} \right) \left(\frac{\partial E}{\partial t} \right) \overline{ut} + \left(\frac{\partial E}{\partial T} \right)^2 \overline{t^2} \quad (2-7)$$

This is the actual equation which would be obtained from a hot wire measurement. For equation (2-7) it is noted that the comparison between the velocity and temperature sensitivity terms goes as the square. Thus, for the mean equation it is evident that the temperature term can be neglected compared to the velocity terms for ΔT greater than about 800°F .

Thus, for flows in which $\overline{ut} = 0$ it is possible to measure the rms longitudinal turbulent velocity in the presence of temperature fluctuations. This is true for the mean quantity only and not applicable for measure of the instantaneous velocity.

For the thermal boundary layer it is by no means evident that $\overline{ut} = 0$. Evidence suggests \overline{ut} is of the order of $\sqrt{u^2} \times \sqrt{t^2}$. Thus, equation (2-7) can at best be written as

$$\overline{e^2} \simeq \left(\frac{\partial E}{\partial V} \right)^2 \overline{u^2} + 2 \left(\frac{\partial E}{\partial V} \right) \left(\frac{\partial E}{\partial t} \right) \overline{ut} \quad (2-7a)$$

for the thermal layer. The measurement of $\overline{u^2}$ and \overline{ut} is made by operating the hot wire at two values of Δt , and solving two simultaneous equations.

Note that the calibration curve of a hot wire for evaluation of both temperature and velocity fluctuations is a three-dimensional curve. Figure 2-7 is a typical calibration curve drawn up a three-dimensional plot. The vertical axis is wire voltage, while the other two axis are flow velocity and temperature difference.

2.42 Evaluation of the turbulent velocities normal to the mean flow. --

To completely evaluate the turbulent fluctuations it is necessary to measure three-components of the turbulent velocity. In the past the normal components of velocity have been evaluated with hot wires yawed to the mean flow direction. Under the present research program the evaluation of turbulence with a yawed hot wire has been experimentally studied. The results are still somewhat sketchy and further work will be done in later programs. In

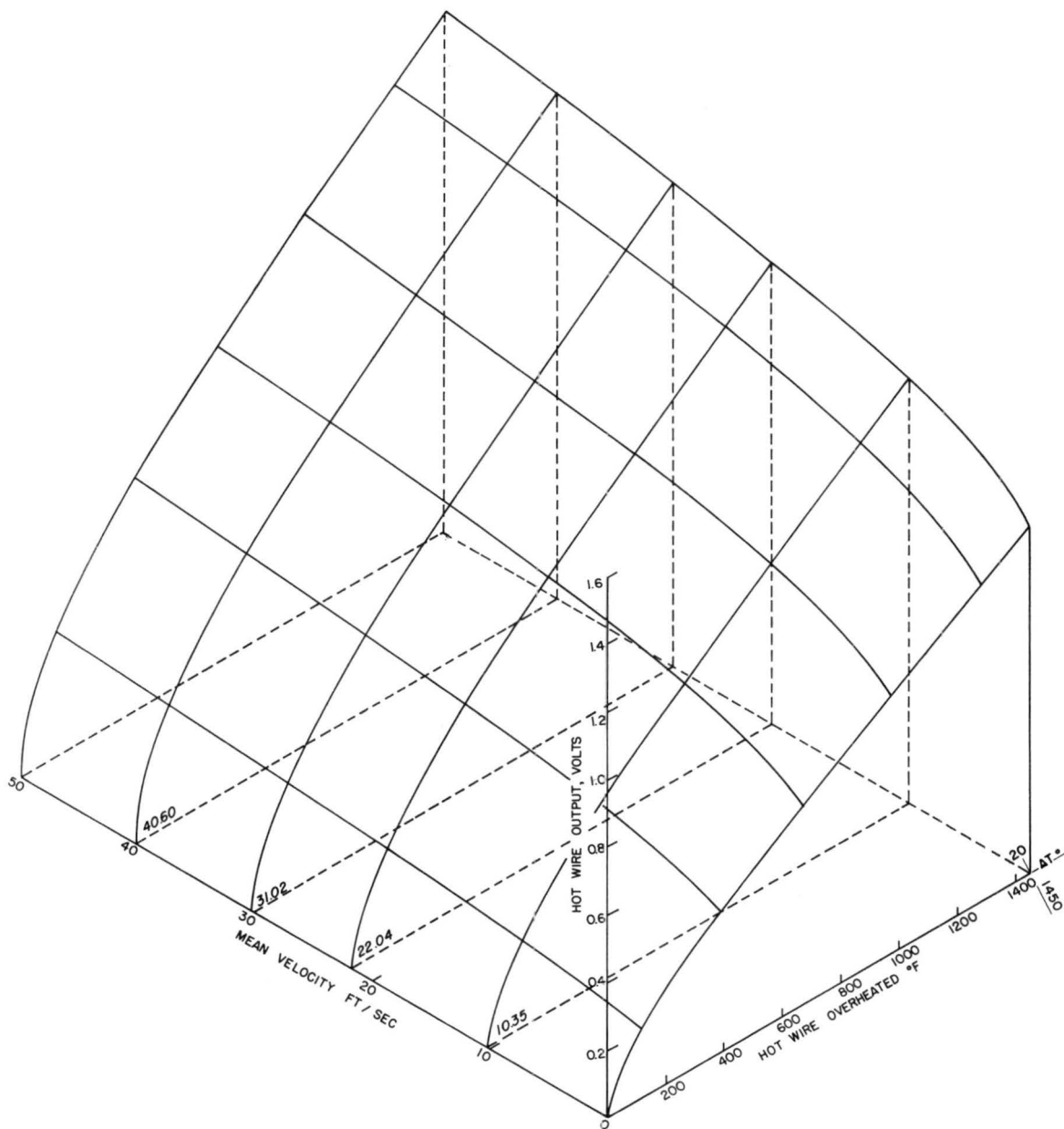


FIG. 2-7. SUMMARY OF HOT WIRE VELOCITY TEMPERATURE CALIBRATION.

general it is found that the problem of the yawed wire is more complex than has been reported in the past. Also it appears that there may be some advantages to operating wire nearly parallel to the mean flow.

Similar to equation (2-5), it is possible to derive an equation between the fluctuating wire voltage and the fluctuation in flow direction.

$$de = \frac{\partial E}{\partial V} dV + \frac{\partial E}{\partial \phi} d\phi \quad (2-8)$$

The fluctuation in flow direction, $d\phi$, can be shown to be approximately equal to: $d\phi \simeq \frac{v}{V_m}$, where v is the normal component of the turbulent velocity in the plane of the wire and V_m is the mean velocity. Thus equation (2-8) may be rewritten as

$$de = \frac{\partial E}{\partial V} dV + \frac{\partial E}{\partial \phi} \frac{v}{V_m} \quad (2-8a)$$

or in terms of perturbations

$$\overline{e^2} = \left(\frac{\partial E}{\partial V} \right)^2 \overline{u^2} + 2 \left(\frac{\partial E}{\partial V} \right) \left(\frac{\partial E}{\partial \phi} \right) \frac{\overline{uv}}{V_m} + \left(\frac{\partial E}{\partial \phi} \right)^2 \frac{\overline{v^2}}{V_m^2} \quad (2-9)$$

There are three turbulent velocity components in equation (2-9) $\overline{u^2}$, \overline{uv} and $\overline{v^2}$, thus it is necessary to make three different measurements to evaluate the terms. Figure (2-8) is a plot of a calibration of a hot wire at different angles, and figure (2-9) is the corresponding three-dimensional calibration curve. As may be seen from figure 2-8 the values of $\frac{\partial E}{\partial V}$ and $\frac{\partial E}{\partial \phi}$ will vary with wire angle. Figure 2-10 shows the variation of $\frac{\partial E}{\partial V}$ and $\frac{\partial E}{\partial \phi}$ with angle for a particular velocity of 20 feet per second. To evaluate the three unknowns the wire would be set to three angles and equation (2-9) would be evaluated at the three conditions. When the wire is normal to the flow equation (2-9) reduces to $\left(\frac{\partial E}{\partial \phi} = 0 \right)$

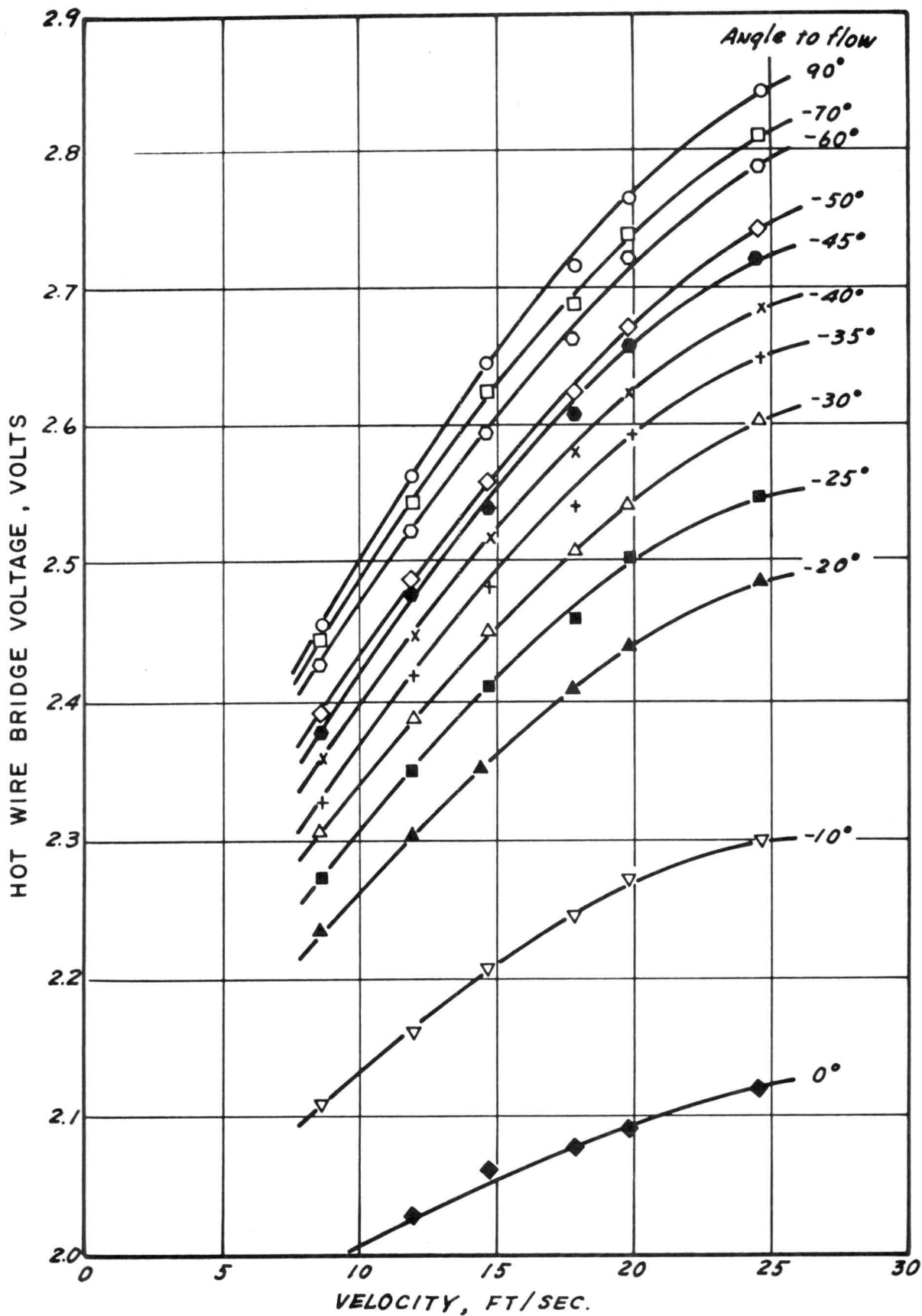


FIG. 2-8 CROSSPLOTS OF PRIMARY CALIBRATION CURVES FOR YAWED HOT WIRE

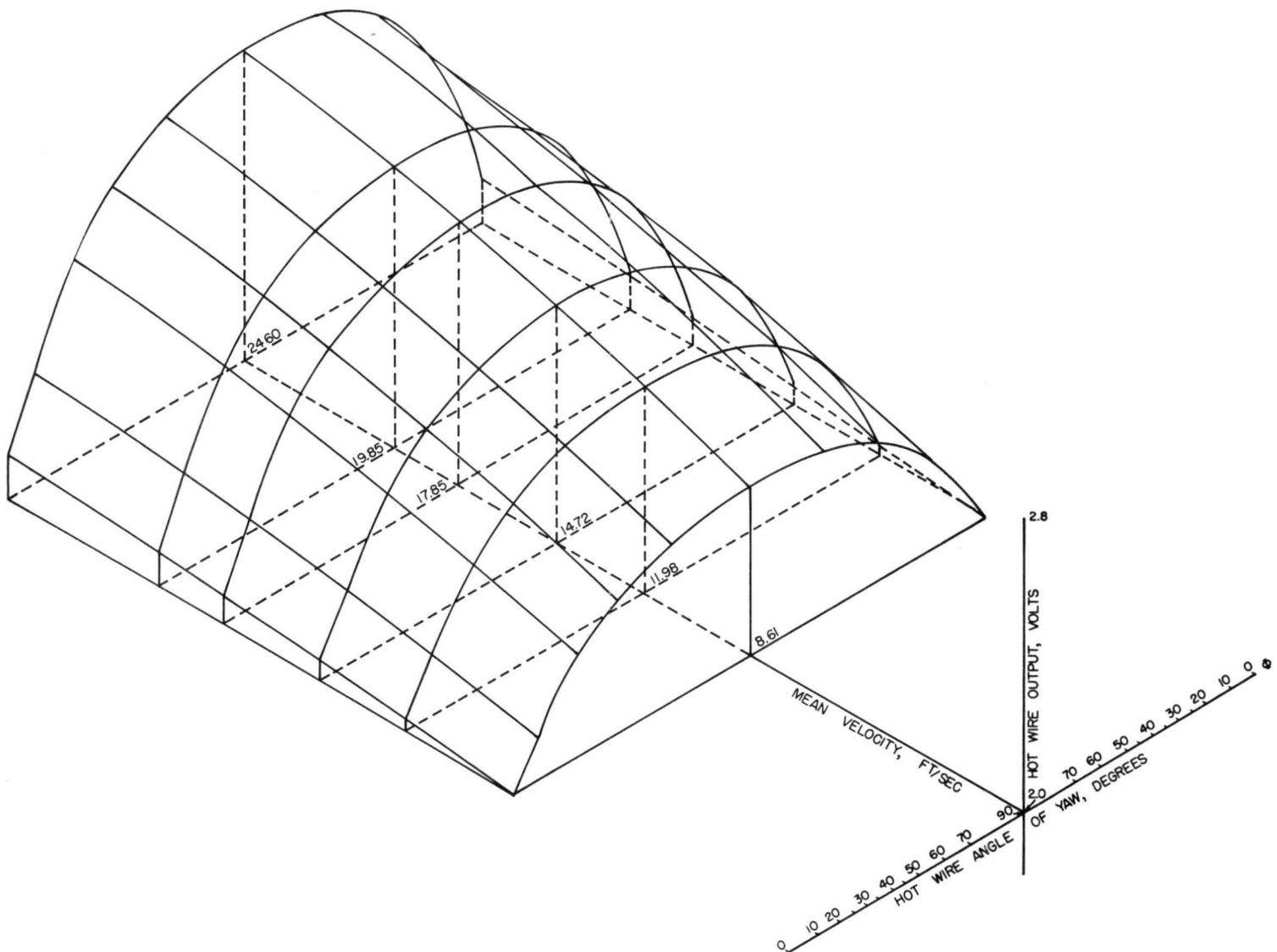


FIG. 2-9. SUMMARY OF YAWED WIRE CALIBRATION.

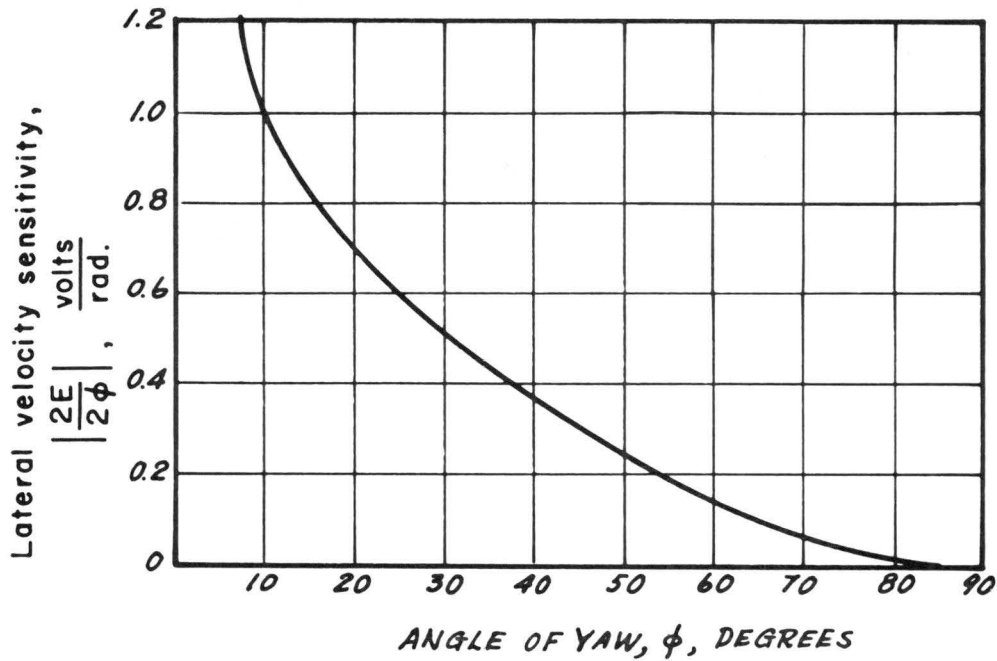
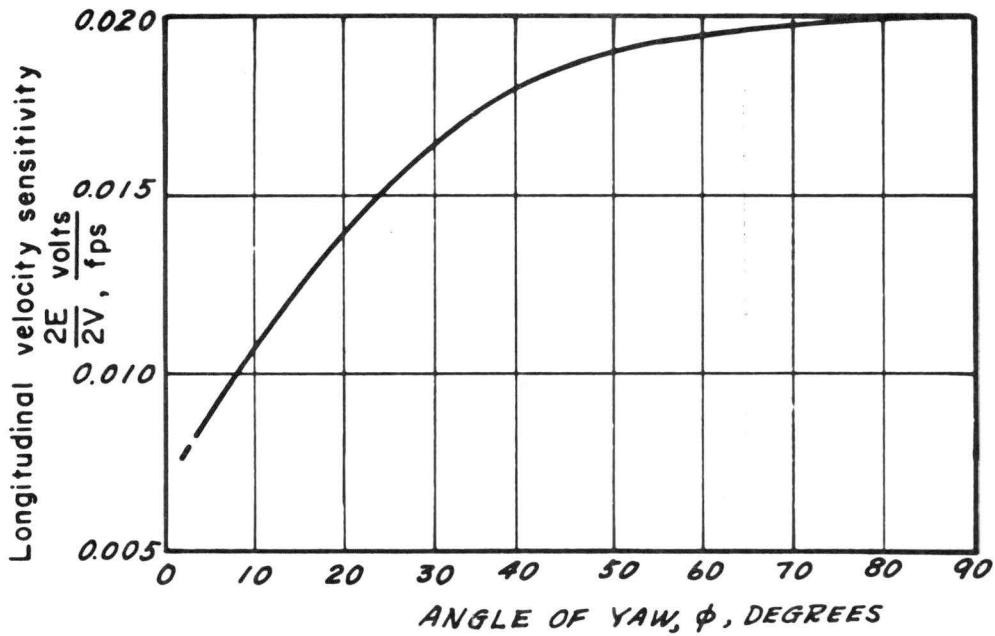


FIG. 2-10 YAWED WIRE SENSITIVITY

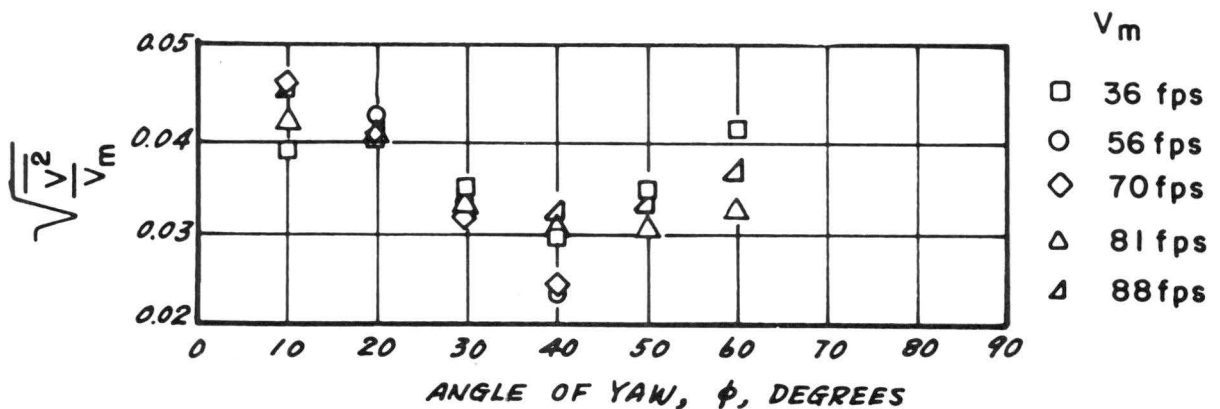


FIG. 2-11 EVALUATED TURBULENT INTENSITY NORMAL TO THE FLOW AS A FUNCTION OF YAW ANGLE

$$\text{NORMAL WIRE } \overline{e^2} = \left(\frac{\partial E}{\partial V} \right)^2 \overline{u^2} \quad (2-10)$$

Thus, $\overline{u^2}$ can be evaluated directly.

A test of the yawed wire analysis was made by evaluating $\overline{v^2}$ from a wire which was rotated to several angles. A plot of $\overline{v^2}$ as a function of yaw angle (for the test $\overline{u^2}$ was evaluated from equation (2-10) and \overline{uv} was zero) is shown in Figure 2-11. The fact that $\sqrt{\overline{v^2}}/V_m$ varies with yaw angle suggests further development of the technique is necessary. In almost every evaluation made to date the minimum value of $\sqrt{\overline{v^2}}$ is found at approximately $\phi = 40^\circ$. The existence of this minimum is not understood. The increase in the computed $\sqrt{\overline{v^2}}$ for small angles is due to an increased effect of the normal velocity component, w , at right angles to the hot wire plane.

A more detailed report on the resistance - temperature transducers will be prepared in the near future. This report will include measurements now in progress.

2.5 Pressure measurements on rough surfaces

The use of pitot tubes and the measurement of pressures near rough boundaries lead to an exploratory study of the pressure distribution about single roughness elements placed closely together along a flat boundary. The study resulted in a paper which has been submitted to the American Society of Civil Engineers for publication in the Proceedings ASCE. The paper has been attached to the report as Appendix 2.

2.6 The calibration of the wind tunnel

2.61 Mean velocity calibration. -- A major portion of the contract time was devoted to a calibration of the large micrometeorological wind tunnel. The unusually long test section, with its square cross section has the tendency to amplify all three dimensional effects, and a uniform velocity distribution within boundary layers along the floor cannot be obtained without appropriate modifications of the wind tunnel.

A series of tests was undertaken with the aim of determining the extent of the non uniformities of the boundary layer flow. A typical set of velocity profiles, taken at an ambient velocity of 20 fps, is shown in Fig. 2-12. The velocity profiles away from the center line are much more convex than the profiles close to the outer line. This is indicative of a secondary circulation pattern in the form of a vortex pair with its axis approximately parallel to the direction of flow. But there is also a marked asymmetry in the flow, and this was attributed to a difference in the location of the transition from laminar to turbulent flow on the sides of the wind tunnel.

To overcome the problem of the corner vortices, a series of fillets were tried out, consisting of 6" or 12" wide plywood sheets placed diagonally across the corners of the test section, but no noticeable improvement was noticed. Equally ineffective were baffles of up to 12" in height placed along the floor at a distance of 18" or 24" from the side walls.

After a great number of experiments with different arrangements of baffles and of trip fences placed at the entrance of the test-section, an

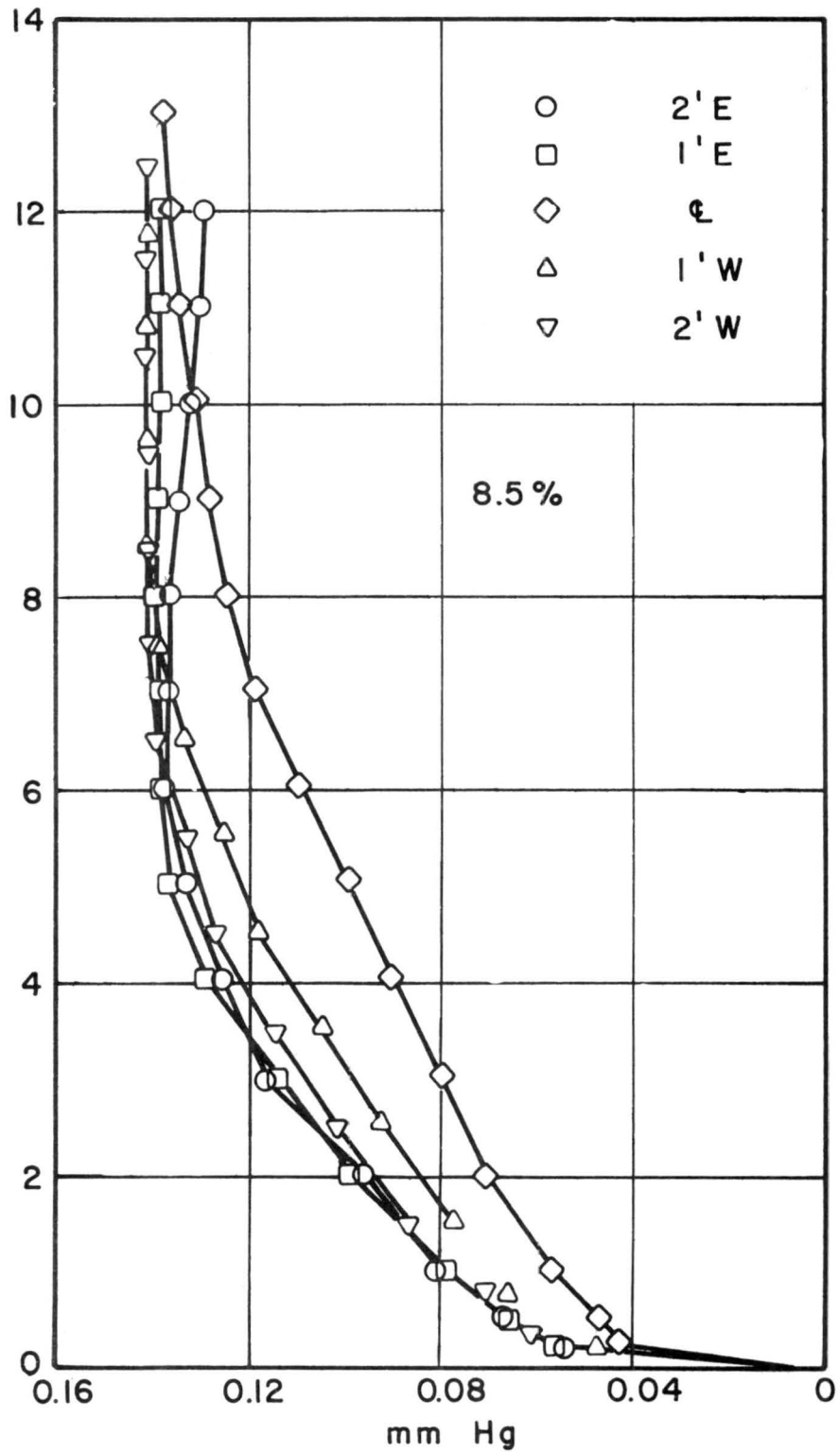


FIG. 2-12 DYNAMIC PRESSURE PROFILES AT STATION 40
 $U_0 = 20$ fps (nominal) before wind
tunnel modification

arrangement was finally found which proved satisfactory to some extent. It consists of a trip fence with saw tooth appearance all around the inlet section. This trip is located at St. 0. It has a height of 1-3/4" on top and bottom, and a height of 1" at the side walls. 3/4" gravel has been placed upwind of the fence, over a distance of 8 ft upwind. Results of the improvements are indicated in Fig. 2-13 which shows dynamic pressure profiles at Sta. 50, that is 10 ft further downstream than the profiles of Fig. 2-12. The improvement is considerable. While the data of Fig. 2-12 give a maximum deviation in velocities about the average local value of approximately $\pm 10\%$, the maximum deviation of the improved set up is less than $\pm 2.5\%$. Also, the data of Fig. 2-12 show the boundary layer thickness across the cross section ranging from about 6" to more than 13". The boundary layer of the improved flow is not only thicker - it is about 15" thick - but it is also practically constant across the cross section of the wind tunnel. A third improvement obtained is the improved symmetry of the flow. The two profiles lying 6" to the East and to the West of the center line are identical, and so are the profiles at 18" from the center line.

2.62 Turbulent intensity calibration. -- A check of the turbulent intensity was made in order to verify that the wind tunnel ambient level of the turbulent intensity is below the level of 0.1% specified in the original contract. The turbulent intensity is defined as the ratio of the root mean square value of the turbulent velocity fluctuations in the axial direction to the free stream velocity u_a . A measurement of the

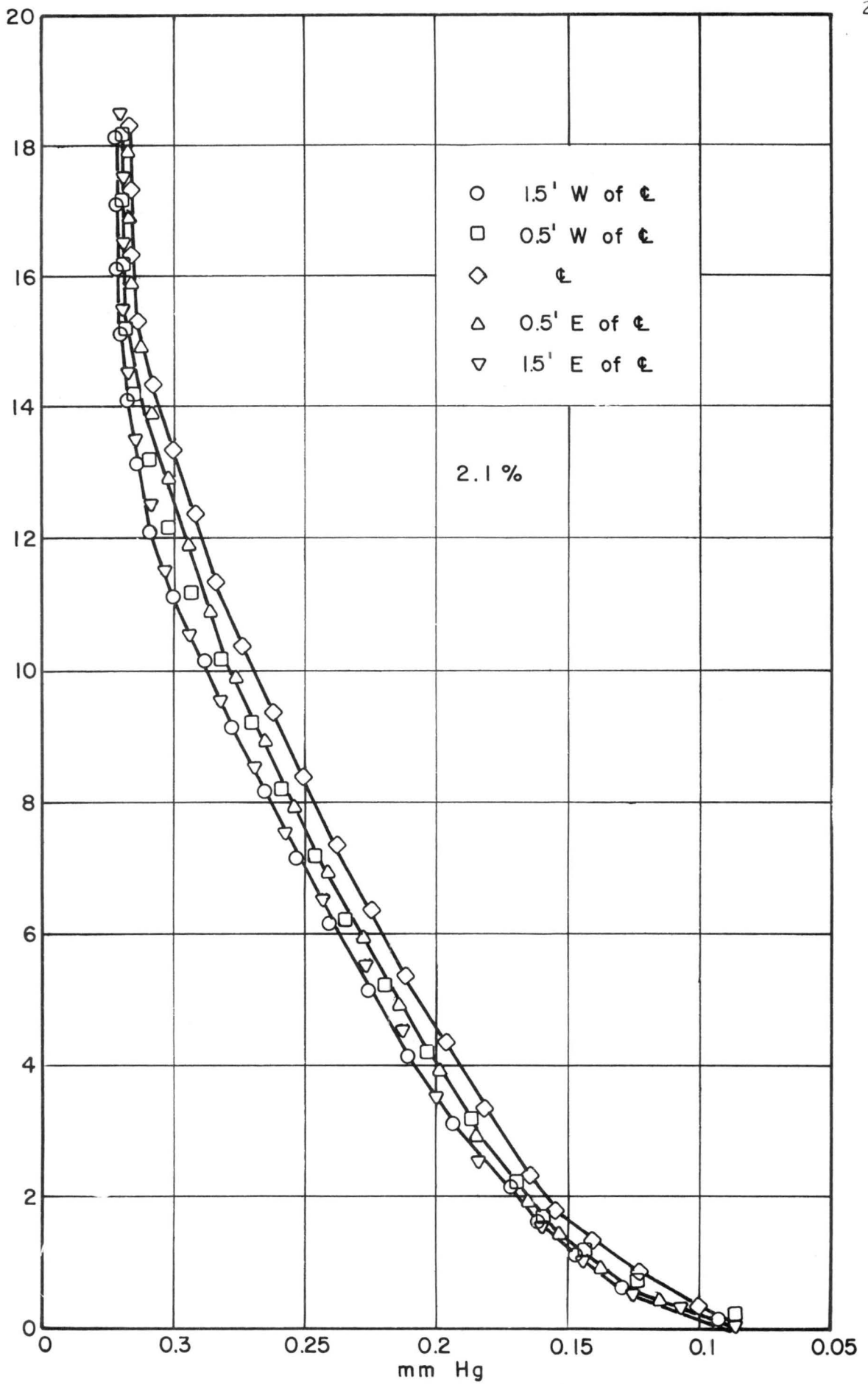


FIG. 2-13 DYNAMIC PRESSURE PROFILES AT STATION 50
 $U_0 = 30$ fps (nominal) after wind tunnel modification

turbulence intensity with the Hubbard Type hot wire anemometer (see ref. 1) gave a value of approximately half of the specified value. However, this signal consists to some part of amplifier noise, i. e. of the error introduced by the electronics of the constant resistance hot wire anemometer amplifier.

In order to check the composition of the turbulent intensity signal, a spectral analysis was made using the Bruel and Kjaer Type 2109 spectrum analyser with a Bruel and Kjaer 2304 recorder. But rather than recording the signal on the 2304 recorder it was preferred to read the rms value of the filter output on a true rms meter, also by Bruel and Kjaer, Type 2409.

The spectral analyses were done by Mr. N. Hwang, under the supervision of Dr. L. V. Baldwin, in the course of a study of the turbulence structure in the wake downstream from a circular disk. A typical example of the spectral density distribution of the square of the turbulent intensity is given in Fig. 2-14 for ambient velocities of 10 and 50 fps. Even though the band width of the filters used is fairly wide ($1/3$ octave filters), it is quite evident that the large peaks except the one at 20 cps correspond to 60 cps or its harmonics - a clear indication of the fact that the major portion of the spectrum is electrical pickup. There is also a second portion, at frequencies larger than 1000 cps, where the energy content is increasing quite sharply. This portion cannot be attributed to turbulence but to the random noise generated by the vacuum tubes and the

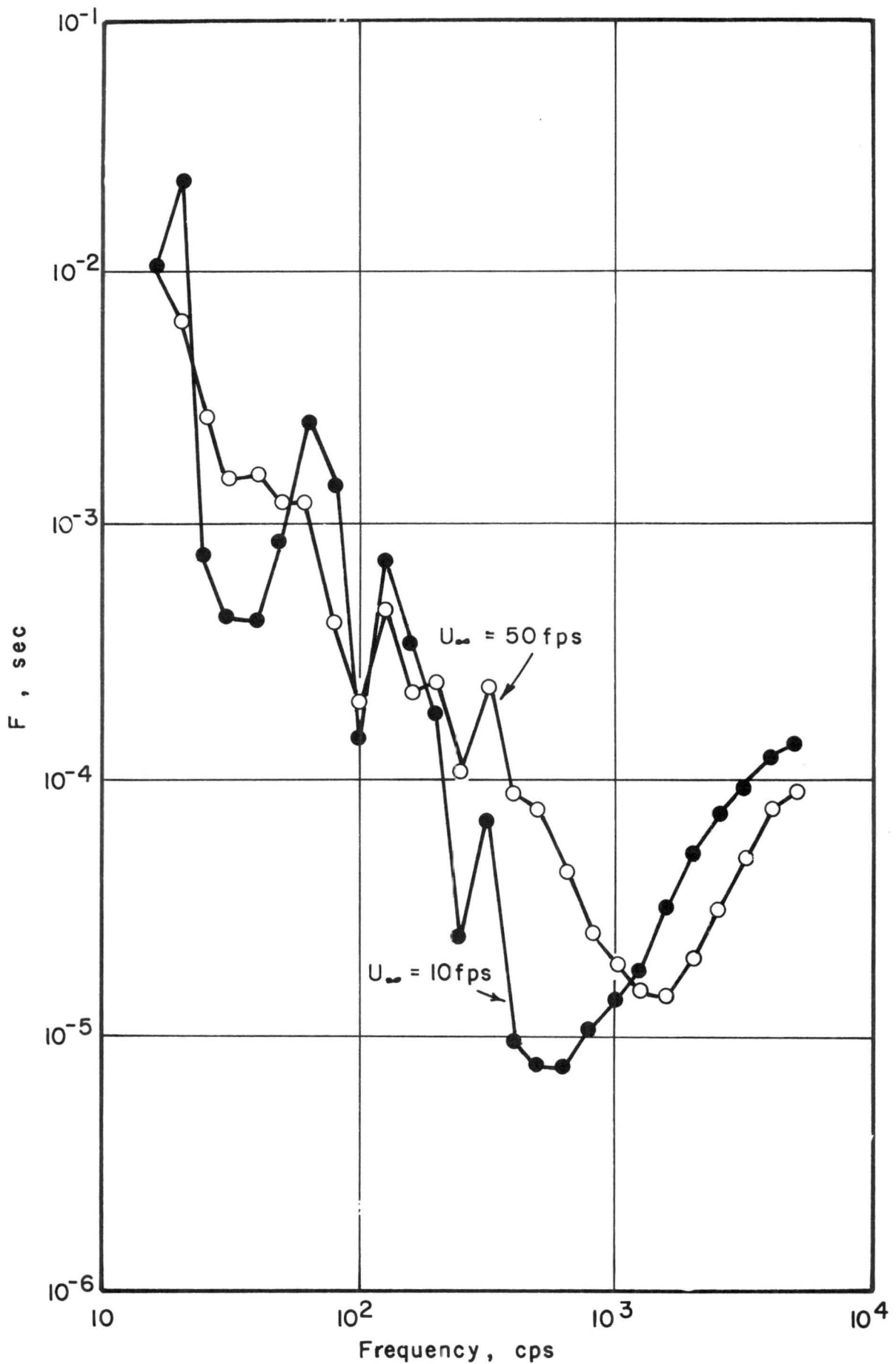


FIG. 2-14 FREESTREAM SPECTRAL DENSITY FUNCTION,
 $U_\infty = 10$ fps vs. $U_\infty = 50$ fps

circuits of the amplifier. It can thus be concluded that the turbulent intensity is well below the design value - in fact, it is below the level which can be measured with any confidence with the instruments which are available in CSU's Fluid Dynamics and Diffusion Laboratory.

2.63 Air temperature calibration. -- The bulb thermometer stretched across the inlet of the wind tunnel test section, as well as a mercury thermometer placed into the free stream of the wind tunnel indicated a cooled air temperature in the test section stable over long periods of time within better than $\pm 1^{\circ}\text{F}$. Fluctuations in the ambient air temperature were measured with a fine wire resistance thermometer. It was found that the signal and noise together had an rms value corresponding to less than $\pm 0.04^{\circ}\text{F}$, and most of the measured fluctuations must certainly be attributed to the instrument noise. Due to difficulties in the heating of the hot brine system, no tests had been made of temperature stability at high temperatures.

2.64 Plate temperature calibrations. -- As is described in ref. 1, the temperature of the temperature controlled, 40 ft long aluminum plate is monitored by thermocouples embedded at 1 ft intervals all along the centerline of the plate. The thermocouples are read out by a multipoint strip chart potentiometer recorder with 24 point print out capability. Since there are 40 thermocouples, they were printed out twenty at a time. The even 20 couples were printed out first, and then, after changing connector plugs, the odd 20 thermocouples.

In testing the temperature stability it was found that there existed no problems with the long range stability of a temperature at a point if no changes in the settings of the electric input heaters, or of the brine flow control valves for the cooling coils underneath the plate were made. However, since changing the setting at one point influences the temperature at the neighboring points, the adjustment of uniform temperatures is a lengthy trial and error procedure. Careful settings of the temperature to within $\pm 1.5^{\circ}\text{F}$ were completed only for one case, that of a plate temperature of 120°F . at an ambient velocity u_a of 30 fps and an ambient temperature T_a of 70°F . For other cases, preliminary settings only were as yet obtained. Some results are shown in Table No. 2. In this table thermocouple "odd 1" is located 1 ft downstream from the leading edge of the plate, and "odd 2, 3, " etc. are each 2 ft apart. Thermocouple "even 1" is located 2 ft downstream from the plate edge, and 2, 3, etc. follow in 2 ft distances. Future heating will be made easier by setting the heating control at the power setting which was read off the monitoring panels on each heater unit. The cold temperatures were obtained with the manual control valves fully open, careful adjustments during which the valve settings will be recorded are required before uniform temperatures are obtained.

TABLE 2. Typical temperature profiles along temperature controlled plate.

Thermo- couple No.	Temperature for case				
	$U_a = 30 \text{ fps } T_a = 70^{\circ}\text{F}$		$U_a = 5 \text{ fps } T_a = 148^{\circ}\text{F}$		
	odd	even	odd	even	odd
1	121	120	220	28	29
2	120	120	220	28	29
3	120	120	221	27	28
4	120	121	224	27	26
5	120	120	220	25	25
6	120	120	222	25	26
7	120	120	223	25	25
8	120	120	215	25	26
9	120	120	220	23	25
10	120	119	213	24	23
11	120	119	217	25	23
12	120	119	217	26	27
13	119	120	220	24	26
14	119	120	220	25	25
15	120	119	217	24	25
16	119	118	215	24	23
17	118	118	220	24	23
18	118	118	220	24	28
19	118	118	217	25	25
20	118	118	218	24	25

III. EXPERIMENTS ON VELOCITY DISTRIBUTIONS OVER NEUTRAL BOUNDARIES

The first series of measurements taken in the wind tunnel were on the velocity distributions along smooth and rough neutral boundaries. For the smooth boundary, the wind tunnel floor was used as it was found after calibration and improvement. The rough boundary was, for a first program on the flow in canopies, made of plastic strips fastened to boards which then were placed on the wind tunnel floor. A short experiment was made on sand roughened plates. For this experiment the plates were 1 ft by 2 ft sheets of masonite covered with the gravel desired and placed on a stand into the ambient air stream 2 ft above the wind tunnel floor.

3.1 Velocity distributions over smooth boundaries

A careful check of the mean velocity profiles along the wind tunnel floor has been made using the continuous recording techniques described in 2.1. Velocity profiles were taken at the center line and at distances from the center line to the East and West as indicated in Table 3. Table 3 also contains a listing of all the stations. Station 0 is at the position of the trip fence, and Stations 10 to 70 are a distance of 10 to 70 ft downstream from Station 0. For the odd decimal stations, 5 profiles were taken and an average formed, so that the recorded profiles represent an average profile across the center portion of the wind tunnel cross section. The likely deviations of the individual profiles from the average are of the order of ± 2 per cent, as was discussed in 2.6. The average profiles are plotted in Fig. 3-1.

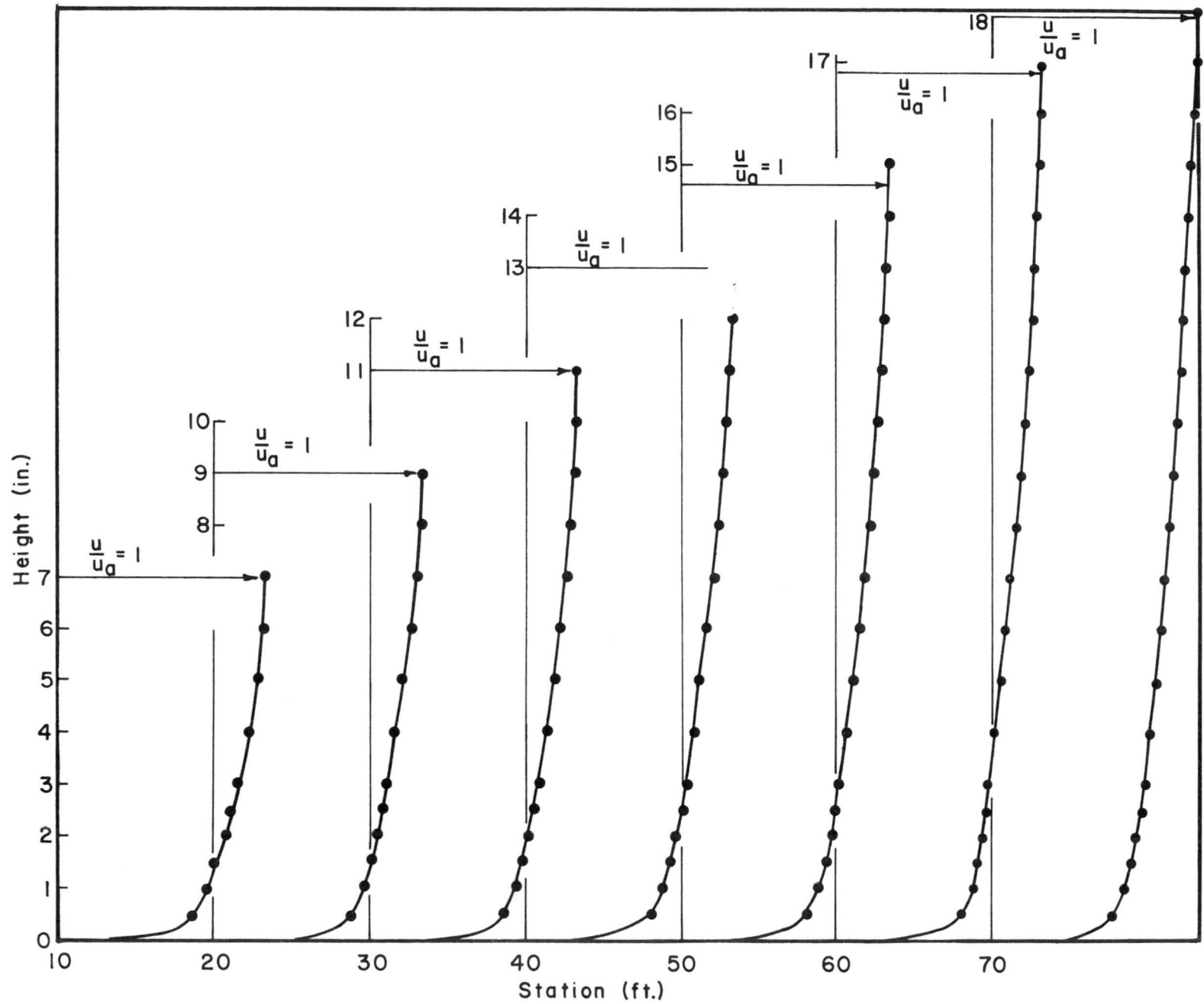


FIG. 3-1 MEAN VELOCITY DISTRIBUTION ALONG CENTER LINE

Table 3. Locations of velocity profiles (profiles were taken at points checked x)

Stat. (ft.)	West of centerline				East of centerline				
	2'	1.5'	1.0'	0.5'	0'	0.5'	1.0'	1.5'	2.0'
10	x		x		x		x		x
20					x				
30	x		x		x		x		x
40					x				
50		x		x	x	x		x	
60					x				
70		x		x	x	x		x	

In order to check whether the profile development along the wind tunnel floor follows that of a smooth flat plate, the profiles were first plotted in non-dimensional form by plotting y/δ vs u/u_a on semi-logarithmic paper. The results are represented in Fig. 3-2. The outer 80 percent of the boundary layer are well described by a "universal" profile, and only in the lower portions do the profiles deviate. The trends are expected. Indeed, according to the recommendations of Hama⁴, the profile along a flat plate is to be composed of four parts: the laminar sublayer close to the wall, a law of the wall, covering a small inner portion of the profile, a velocity defect law in the form

$$\frac{u_a - u}{u_*} = f\left(\frac{u_* y}{\nu}\right) \quad (3-1)$$

⁴F. R. Hama (1954), "Boundary layer characteristics for smooth and rough surfaces," Trans. Soc. Naval and Marine Architects, Vol. 62, pp. 333-358.

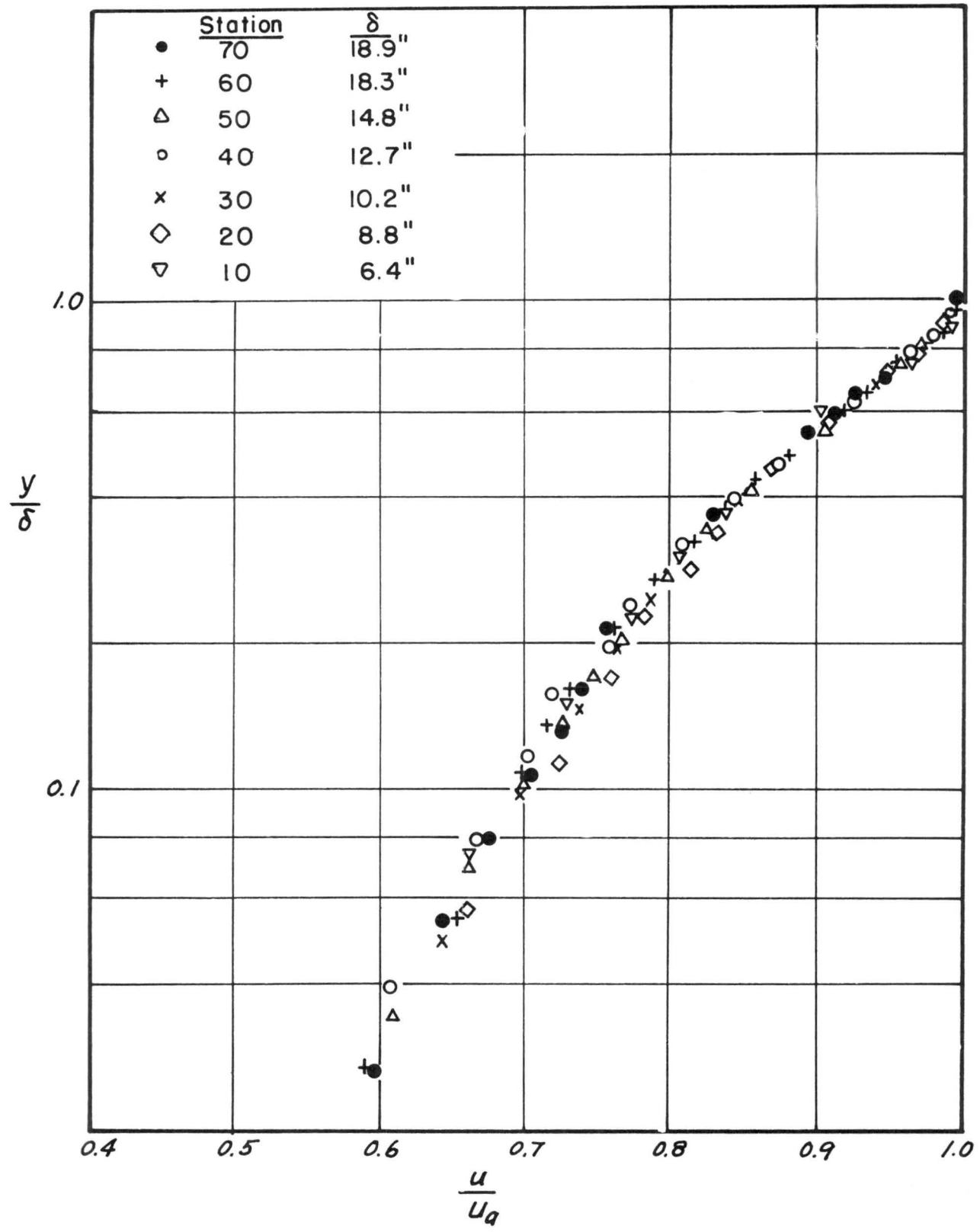


FIG. 3-2 NON-DIMENSIONAL VELOCITY PROFILES: THE LAW OF DEFECT IN THE OUTER FLOW

and an outer portion depending on the boundary layer thickness, and given by Hama⁴ in the form

$$\frac{u_a - u}{u_*} = -9.6 \left(1 - \frac{y}{\delta}\right)^2 \quad (3-2)$$

The data have not been taken as close to the wall as necessary to verify the wall law and the velocity distributions in the viscous sublayer. However, the law of the wall has been found to exist in almost all turbulent boundary layer flows, in all types of pressure gradients (for example, Coles⁵ and Clauser⁶).

The data in the middle region follow the velocity defect law as given by Clauser⁶ and reproduced by Hinze⁷. This is evident from Fig. 3-3. In this plot, the shear stress at the wall was assumed approximately constant for all x . For a smooth flat plate, the shear stress depends on the Reynolds number, and the standard graph of friction factors vs Reynolds No. (for example Schlichting⁸, p. 538) gives friction factors of from 3.1×10^{-3} to 2.6×10^{-3} for the Reynolds No. range corresponding to the experimental data. The measured value is approximately 2.7×10^{-3} .

The data in the outer region do not agree with those of Hama⁴. The data are too well in agreement with each other for assuming the deviation

⁵D. Coles (1956), "The law of the wake in the turbulent boundary layer", Journ. Fluid Mech., Vol. 1, p. 191-226.

⁶F. Clauser, (1956), "The turbulent boundary layer," in Vol 4, Advances in Applied Mechanics, Academic Press, New York, p. 2-51.

⁷J. O. Hinze (1959), "Turbulence," McGraw Hill, New York.

⁸H. Schlichting (1960), "Boundary layer theory," McGraw Hill, New York.

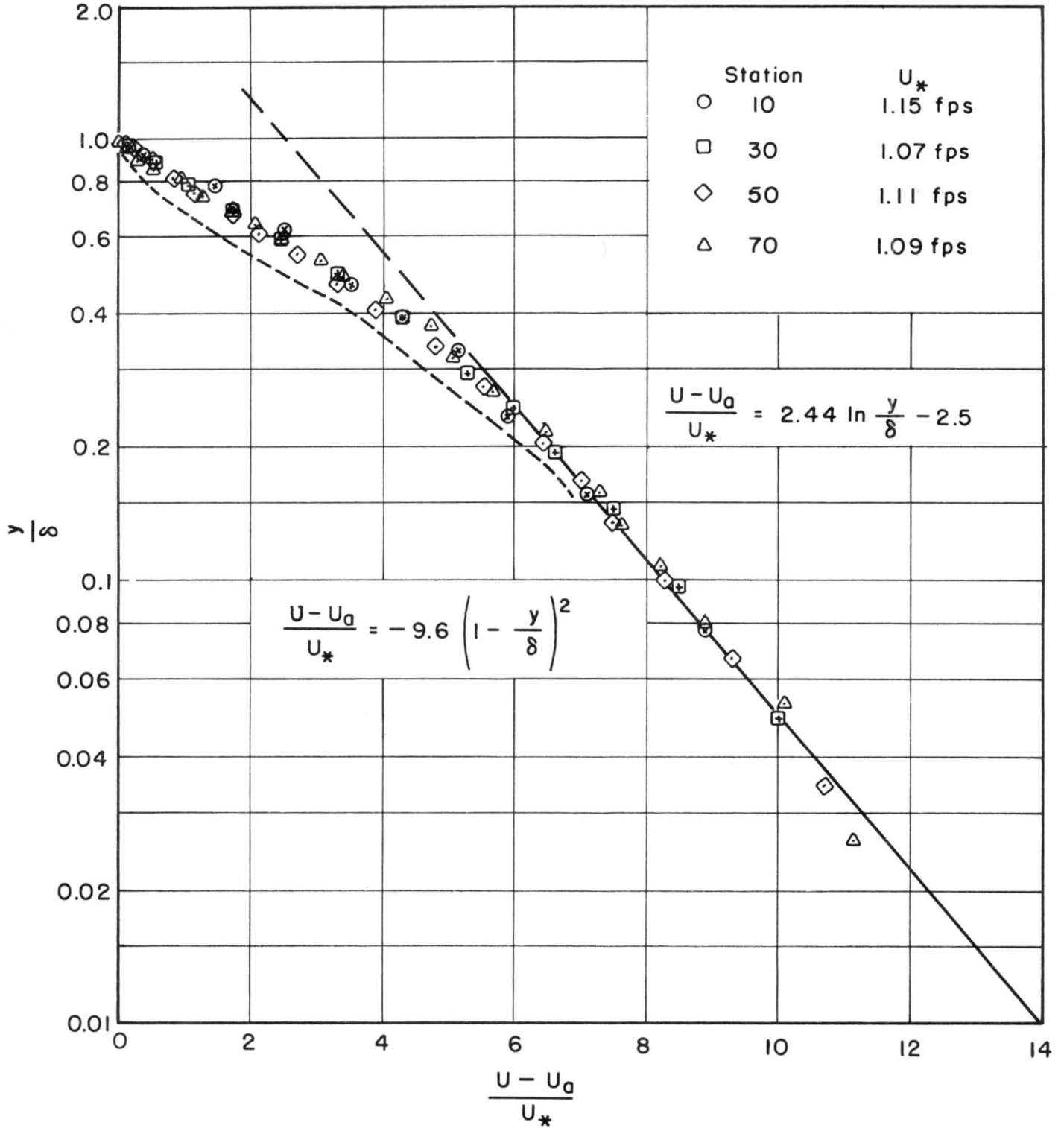


FIG. 3-3 COMPARISON OF EXPERIMENTAL DATA
WITH FORMULAS OF HINZE () p. 480

to be measurement error, unless the error is systematic. An extended program is planned in which the shear stress at the wall will be measured directly which will take the guess out of the determination of the shear velocity.

There is another oddity in the experimental data, and this is the development of the boundary layer. Blasius' formula⁸ for the boundary layer thickness is given by

$$\delta = 0.37 x \left(\frac{u_a x}{\nu} \right)^{-1/5} \quad (3-3)$$

where x is the distance from the plate leading edge and ν the kinematic viscosity. For using the floor of the wind tunnel as the plate, an origin has to be defined for x which is not the entrance of the test section but somewhat more upstream. It was chosen in such a way as to make the exponent in the power law relationship Eq. 3-3 to agree with the experimental data. This yielded an origin located about 10 ft upstream from Sta. 0. With this origin for x , the experimental data were plotted on double logarithmic paper in Fig. 3-4. The resulting equation

$$\delta = 0.52 \cdot x \left(\frac{u_a x}{\nu} \right)^{-1/5}$$

agrees with Eq. 3-3 except in the coefficient 0.52 instead of 0.37. This difference must be attributed to the artificial roughening of the test section floor at the entrance.

3.2 Velocity distributions over sand roughened boundaries

For investigating the turbulence structure very near a rough boundary it was not considered necessary to roughen the whole test section floor.

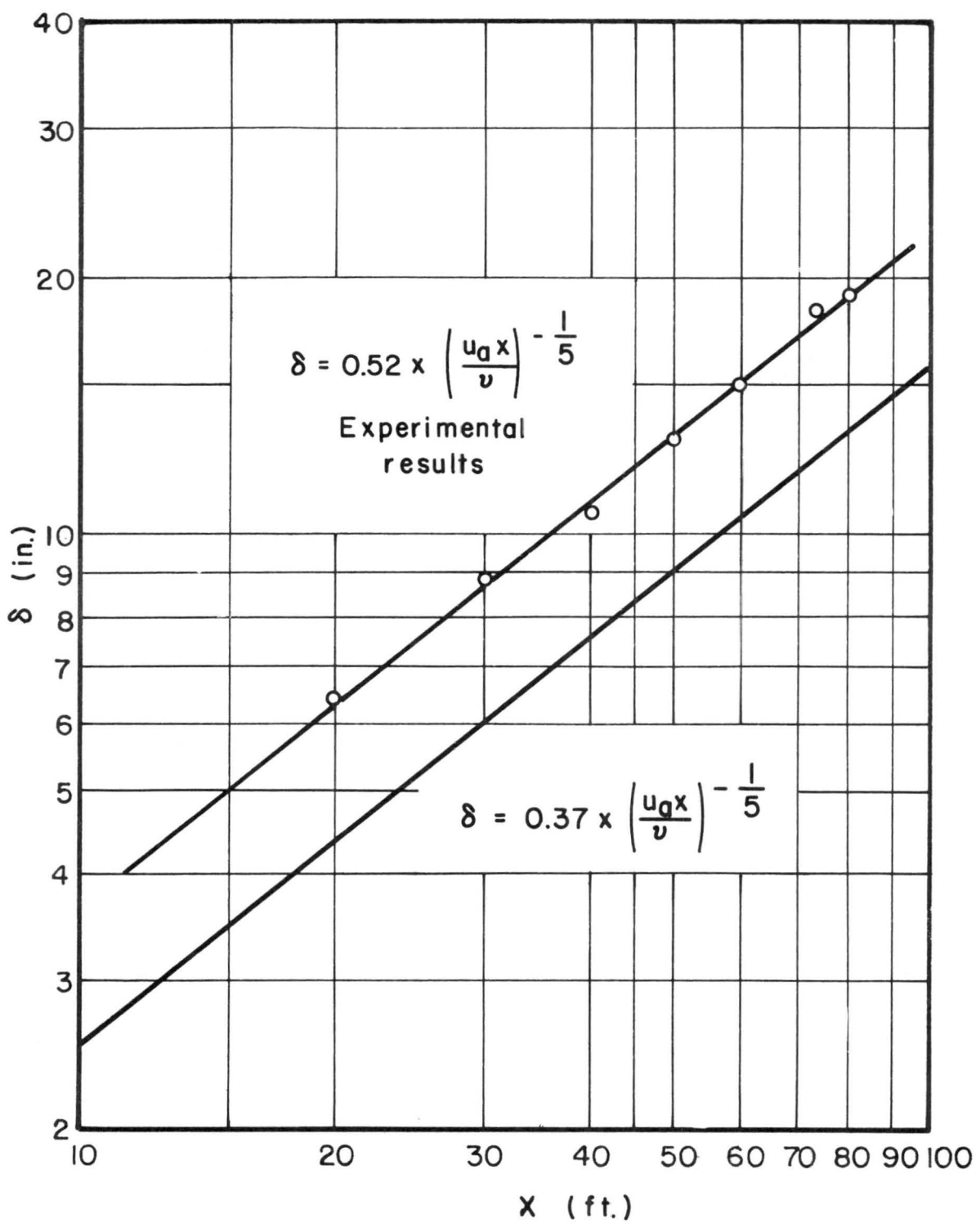


FIG. 3-4 BOUNDARY LAYER DEVELOPMENT

Instead, small plates 1 ft by 2 ft were made of masonite and covered with sand. The properties of the sand roughnesses are listed in Table 4. Velocity profiles were measured at distances of 10, 13, 16, and 18 inches from the blunt edge; the profile parameters calculated from the velocity profiles are summarized in Table 5. An inspection of the parameters revealed that equilibrium had probably nowhere been reached, and an improved experimental set up will be used for future experiments in which the plate is 3 ft wide and 6 ft long, the pressure gradient along the plate is accurately controlled, and the two dimensionality of the flow across the plate is carefully checked. The experimental roughnesses used for these preliminary experiments will however, be used also for the improved tests.

TABLE 4

Plate	No. 1	No. 2	No. 3	No. 4
Average size of grains in mm	3.66 mm	1.55 mm	0.61 mm	0.28 mm
Number of grains per cm ²	4.34	36.6	280	1240

3.3 Velocity distributions inside and above flexible roughness

A first completed study of the velocity distributions in the Army Micrometeorological Wind Tunnel is that on the velocity distributions inside and above a rough boundary consisting of flexible roughness elements. The elements and their arrangements are shown in Fig. 1-6 of Appendix 3. The results of this study were presented in a dissertation by

TABLE 5

Roughness Type	u_{amb}	Station	δ''	δ^*''	θ''	H
No. 1	19.8	10	1.227	.2664	.1764	1.510
		13	1.330	.2773	.1895	1.462
		16	1.436	.2961	.2042	1.450
		18	1.528	.3157	.2202	1.437
No. 2	20.5	10	1.150	.2309	.1588	1.453
		13	1.250	.2501	.1754	1.425
		16	1.354	.2570	.1845	1.393
		18	1.450	.2665	.1950	1.365
No. 3	19.8	10	1.030	.1610	.1224	1.314
		13	1.132	.1736	.1344	1.290
		16	1.240	.1877	.1469	1.276
		18	1.330	.2022	.1594	1.267
No. 4	19.5	10	1.050	.1710	.1242	1.376
		13	1.150	.1757	.1327	1.331
		16	1.250	.1895	.1454	1.302
		18	1.351	.2066	.1615	1.278
No. 2	42.0	10	.870	.2129	.1382	1.541
		13	.982	.2356	.1528	1.540
		16	1.083	.2702	.1768	1.529
		18	1.182	.3064	.1978	1.549
No sand	21.0	13	.853	.1312	.1012	1.297
		16	.950	.1501	.1105	1.359
		18	1.052	.1637	.1249	1.310

A. A. Quraishi⁹. An investigation of the equilibrium profiles which occur at a large distance downstream from the leading edge of the roughness cover was made in a paper by Plate and Quraishi which was submitted for publication to the Journal of Applied Meteorology. This paper is attached to the report as Appendix 3. An investigation of the flow pattern in the region just downstream from the roughness elements will be made during the continuation of the program.

IV. EXPERIMENTS ON VELOCITY DISTRIBUTIONS OVER HEATED BOUNDARIES

A series of preliminary experiments has been made in order to develop experience with the techniques to be used for measuring temperature and velocity distributions in stratified flows. The measurements of mean velocity profiles presents no additional problem, except that the data will have to be corrected for density changes depending on the temperature distributions. The temperature distributions are not measured with the same convenience; a first set of data obtained for the temperature distribution are almost certainly contaminated by transient response errors of the thermocouple used for taking the profiles. This lead to the investigation reported in 2.2 and 2.3. The transient errors will, however, be minimized in the outer regions of the temperature boundary layer. Therefore, the only conclusions of some validity that can be drawn concern the development of the thermal boundary layer. A unique curve for the ratio of the thermal boundary layer to the momentum boundary layer does seem to

⁹A. A. Quraishi (1963), "Effects of flexible roughness elements on diffusion in a turbulent boundary layer," Ph.D. Dissertation, Colo. State Univ., Fort Collins, Colo., 189 p.

exist, as shown in Fig. 4-1. An extensive search of the literature on the development of thermal boundary layers which was initiated for the purpose of finding data to compare the present experimental results did not bring forth any directly applicable results. Eckert and Drake¹⁰ cover the laminar equivalent of the case and give an equation for the ratio of the two boundary layer thicknesses which is also shown in Fig. 3-1. Further work is in progress on the properties of thermally stratified boundary layers.

¹⁰E. R. G. Eckert and R. M. Drake, Jr. (1959), "Heat and Mass Transfer," McGraw Hill, New York.

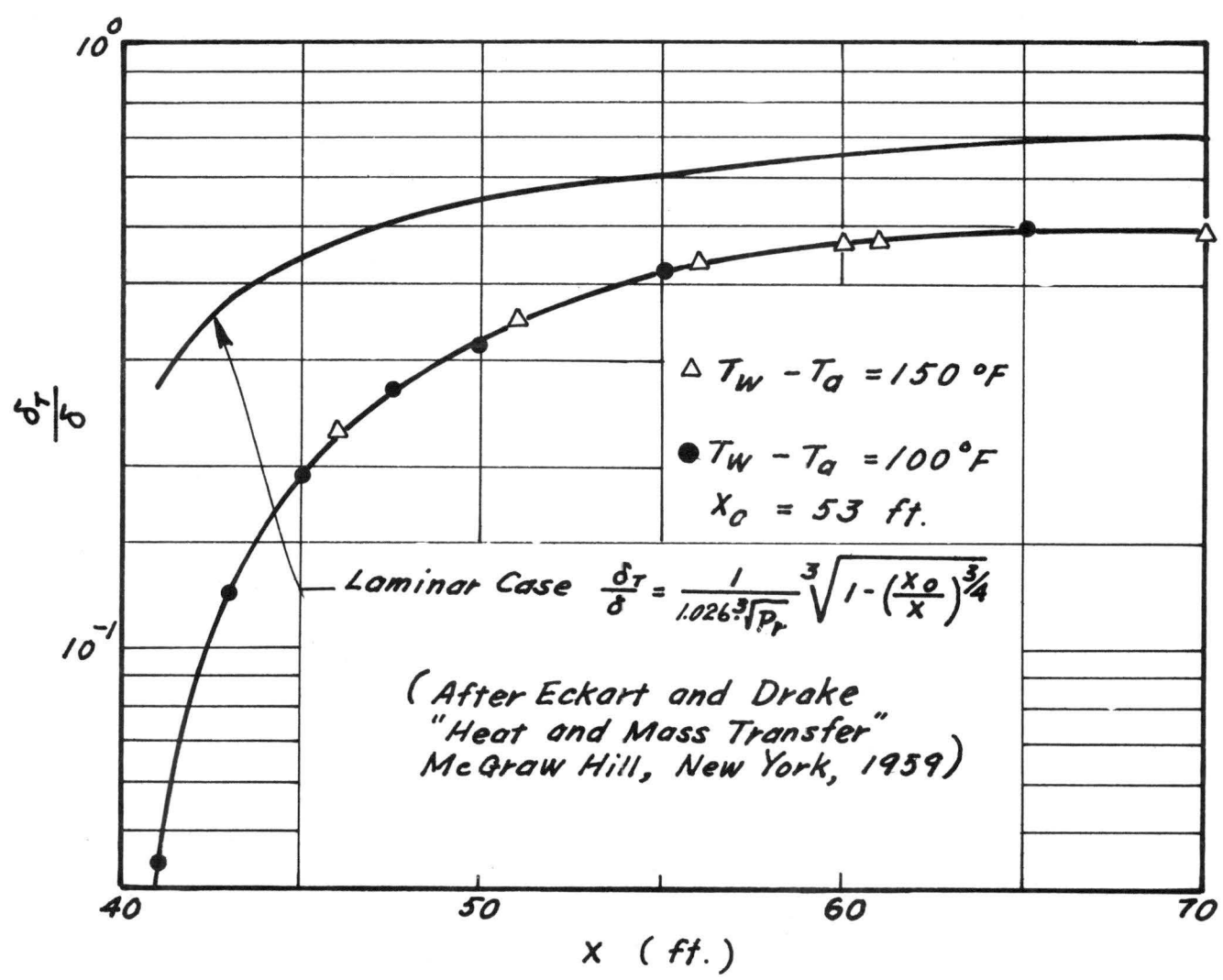


FIG 4-1 RATIO OF THERMAL BOUNDARY LAYER TO FLOW BOUNDARY LAYER